

1 **NCED expression is related to increased ABA biosynthesis and stomatal closure under**
2 **aluminum stress**

3

4

5 Marina Alves Gavassi¹, Giselle Schwab Silva¹, Carolina de Marchi Santiago da Silva², Andrew
6 J. Thompson³, Kyle Macleod³, Paulo Marcelo Rayner Oliveira⁴, Mariana Feitosa Cavalheiro⁵,
7 Douglas Silva Domingues⁶, Gustavo Habermann^{6*}

8

9 ¹*Programa de Pós-Graduação em Biologia Vegetal, Departamento de Biodiversidade,*
10 *Instituto de Biociências, Universidade Estadual Paulista, UNESP, Av. 24-A, 1515; 13506-900,*
11 *Rio Claro, SP, Brazil;* ²*Departamento de Ciências Biológicas, Escola Superior de Agricultura*
12 *“Luiz de Queiróz” Universidade de São Paulo, ESALQ-USP, Av. Pádua Dias, 11, 13418-900,*
13 *Piracicaba, SP, Brazil;* ³*Cranfield Soil and Agrifood Institute, Cranfield University, College*
14 *Rd, MK43 0AL, Cranfield, United Kingdom;* ⁴*Departamento de Botânica, Instituto de*
15 *Biociências, Universidade de São Paulo, USP, Rua do Matão, 14, 05508-090, São Paulo - SP,*
16 *Brazil;* ⁵*Programa de Pós-Graduação em Genética e Biologia Molecular, Centro de Biologia*
17 *Molecular e Engenharia Genética, Instituto de Biologia, Universidade Estadual de Campinas,*
18 *Avenida Cândido Rondon, Cidade Universitária, 13083875, Campinas, SP, Brazil*
19 ⁶*Departamento de Biodiversidade, Instituto de Biociências, Universidade Estadual Paulista,*
20 *UNESP, Av. 24-A, 1515; 13506-900, Rio Claro, SP, Brazil.*

21 * Author for correspondence: Gustavo Habermann, Tel: +0055 (19) 3526-4210,
22 gustavo.habermann@unesp.br

23

24

25 **ABSTRACT**

26 Aluminum (Al)-induced decrease in leaf hydration has been associated with low gas exchange,
27 especially stomatal conductance (g_s). However, the mechanisms explaining these responses are
28 unclear. *Citrus limonia* was exposed to 0 and 1480 μ M Al in nutrient solution for 90 days to
29 test whether the low g_s and leaf hydration in plants exposed to Al is associated with increased
30 9-*cis*-epoxycarotenoid dioxygenase (NCED) gene expression and abscisic acid (ABA)
31 biosynthesis. Relative leaf water content (RWC), water potential (Ψ_w) and gas exchange in
32 the leaves, as well as leaf and root *CINCED3*, *CINCED1* and *CINCED5* expression and
33 accumulation of ABA and its metabolites (phaseic acid, dihydrophaseic acid, (+)-7'-hydroxy-
34 ABA and ABA- β -D-glucosyl ester) were measured. Al up-regulated *CINCED3* and induced
35 ABA accumulation in the roots before impairments in leaf water status (low Ψ_w , RWC and
36 g_s) could be observed. Leaf ABA concentration increased from 7 to 90 days and this could be
37 partially explained by the up-regulation of *CINCED3*, *CINCED1* and *CINCED5* in this organ.
38 Stomatal closure occurred concomitantly with the increase of ABA concentration, and this
39 result provides further evidence of the role of ABA modulation of plant hydration under Al
40 stress.

41

42 **Keywords:** ABA, aluminum, *Citrus*, plant signalling, water relations, NCED genes

43

44

45 **1. Introduction**

46 Several studies have shown low stomatal conductance (g_s) in plants under aluminum
47 (Al) toxicity. In comparison to plants not exposed to Al, g_s values may reduce by 80% in
48 *Solanum lycopersicum* (Simon et al., 1994) and *Secale cereale* (Silva et al., 2012), 44% in *Zea*
49 *mays* (Anjum et al., 2016), 38% in *Hordeum vulgare* (Ali et al., 2011), 30% in *Citrus reshni*
50 ('Cleopatra' tangerine) (Chen et al., 2005b), 40% in *C. grandis* ('Sour Pummelo') (Jiang et al.,
51 2008) and 50% in *C. limonia* ('Rangpur' lime) (Silva et al., 2018).

52 As g_s is controlled tightly by plant water status (Dodd et al., 2003; Huber et al., 2019),
53 one explanation for the low g_s in plants exposed to Al could be the inhibition of root growth
54 (Kopittke et al., 2008; Singh et al., 2017; Silva et al., 2019). Al-induced reduction in g_s is
55 considered an indirect (long distance) effect of Al because it is nearly all retained in negatively
56 charged pectin nets of root cells (Kopittke et al., 2015). Thus, Al toxicity results in lower root
57 surface area (Panda et al., 2009; Szatanik-Kloc, 2016), reduction in water uptake, water
58 deficiency in the shoot (Tamás et al., 2006; Yang et al., 2013) and low g_s (Vitorello et al.,
59 2005). However, most studies in which Al induced low g_s (Simon et al., 1994; Jiang et al.,
60 2008; Ali et al., 2011; Silva et al., 2012; Banhos et al., 2016; Silva et al., 2018; Cavaleiro et
61 al., 2020) were conducted with plants growing directly on nutrient solution, where water is
62 constantly available. In addition, fibrous xylem vessels (Banhos et al., 2016), more lignin
63 deposition (Silva et al., 2019) and structural damage (Batista et al., 2013) to the root vascular
64 cylinder have been observed in plants under Al toxicity. Aluminum also decreases root
65 hydraulic conductivity in maize plants maintained in nutrient solution (Gunsé et al., 1997),
66 although this study did not measure g_s and neither associated both variables. Furthermore, low
67 leaf water potential (Ψ_w) and decreased relative leaf water content (RWC) can be observed in
68 plants exposed to Al, even when the plants are grown directly on nutrient solution (Banhos et
69 al., 2016; Silva et al., 2018; Cavaleiro et al., 2020).

70 Besides low root growth and compromised plant hydraulics, root-to-shoot chemical
71 signalling could also explain low g_s in plants exposed to Al in nutrient solution. For example,
72 abscisic acid (ABA) signalling controls g_s when roots are exposed to Al, but only few studies
73 have examined the role of ABA in plants exposed to Al, and these studies have focused on the
74 role of ABA in root Al resistance, without measuring g_s (Shen et al., 2004; Hou et al., 2010;
75 Reyna-Llorens et al., 2015; Kopittke, 2016). Recent evidence showed that decrease in root
76 hydraulic conductance and increase in ABA could explain Al-induced stomatal closure in
77 tomato plants (Gavassi et al., 2020). ABA strongly controls stomatal movement (Zhang and
78 Davies, 1989; Merilo et al., 2015), and stomatal closure is one of the most studied roles of

79 ABA in response to drought, high temperature and salt stress (Xiong and Zhu, 2003; Mehrotra
80 et al., 2014). In plants under drought, ABA rapidly accumulates causing low g_s to reduce
81 transpiration (Zhang et al., 2008; Estrada-Melo et al., 2015). Cellular ABA concentration
82 continuously fluctuates, enabling plants to grow while coping with stressful conditions (Ma et
83 al., 2018). ABA concentration is regulated by its biosynthesis (Ng et al., 2014), which
84 originates from the cleavage of xanthophyll precursors, and also its degradation (Xu et al.,
85 2013). The main oxidative route of ABA catabolism is the 8' hydroxylation, which produces
86 8'-hydroxy-ABA (Cutler and Krochko, 1999). This compound isomerizes to phaseic acid (PA),
87 which may be reduced to dihydrophaseic acid (DPA) (Okamoto et al., 2009). A minor
88 oxidative route produces (+)-7'-hydroxy-ABA (7'OHABA), whereas a minor reductive
89 pathway produces an unstable 1',4'-diol ABA. ABA and its metabolites may also be conjugated
90 with glucose to form ABA- β -D-glucosyl ester (ABA-GE) (Zaharia et al., 2005).

91 The enzyme 9-*cis*-epoxycarotenoid dioxygenase (NCED) catalyzes the rate-limiting
92 step in ABA biosynthesis (Thompson et al., 2000). This gene encoding NCED form a small
93 multigene family containing five members (*NCED2*, 3, 5, 6, 9) in *Arabidopsis thaliana* (Tan
94 et al., 2003), and *NCED3* is mainly responsible for ABA accumulation under drought stress in
95 *Arabidopsis* (Iuchi et al., 2001). *NCED3* has been demonstrated to act with *NCED5* against
96 drought stress (Frey et al., 2012). Over-expression of *NCED* leading to ABA over-
97 accumulation was first achieved in tomato and tobacco (Thompson et al., 2000); in tomato this
98 increased root hydraulic conductivity and lowered g_s , resulting in higher water use efficiency
99 (Thompson et al., 2007). In *Citrus*, when an *NCED3* ortholog, *CrNCED1*, was isolated from
100 'Cleopatra' mandarin (*Citrus reshni*) and overexpressed in transgenic tobacco, the plants
101 showed higher levels of ABA and enhanced tolerance against drought, salt, and oxidative
102 stresses when compared with WT (Xian et al., 2014). Although *NCED* genes have been well
103 characterized in model plants under water deficiency (Xian et al., 2014), their responses in
104 plants exposed to Al remain unknown.

105 As Al reduces g_s by a mechanism not yet elucidated, it is possible that Al toxicity alters
106 *NCED* expression and the plant accumulates more ABA when compared to those not exposed
107 to Al. Here we tested whether 1480 μ M Al (40 mg L⁻¹), an Al concentration that reduces g_s in
108 *Citrus* plants (Banhos et al., 2016; Cavalheiro et al., 2020), also up-regulates *NCED1*, *NCED3*
109 and *NCED5*, and promotes ABA accumulation in roots and leaves of *C. limonia*. Furthermore,
110 we sought to elucidate if ABA biosynthesis is induced before or after the reduction in leaf
111 hydration, evidenced by low Ψ_w , RWC and g_s .

112

113 **2. Material and methods**

114 **2.1. Plant material and experimental conditions**

115 Seventy-two three-month-old and 15 ± 1 cm-high ‘Rangpur’ lime plants (*Citrus*
116 *limonia* L.) were used for studying the plant hydration capacity when subjected to Al within a
117 90-day period. This species is an important rootstock for rain-fed *Citrus* plantations due to its
118 high drought resistance (Banhos et al., 2016). At the beginning of the study, the plants had five
119 leaves and were grown directly on an aerated nutrient solution inside opaque plastic boxes (50
120 cm in length x 30 cm in width x 15 cm in height; 20 L), with six plants per box, in a greenhouse.

121 The nutrient solution used was based on the solution proposed by Clark (1975), and it
122 has been used to test Al tolerance in *C. limonia* (Banhos et al., 2016; Silva et al., 2018; Silva
123 et al., 2019; Cavalheiro et al., 2020). It contained 1372.8 μM $\text{Ca}(\text{NO}_3)_2$, 507.0 μM NH_4NO_3 ,
124 224.4 μM KCl , 227.2 μM K_2SO_4 , 218.6 μM KNO_3 , 483.2 μM $\text{Mg}(\text{NO}_3)_2$, 12.9 μM KH_2PO_4 ,
125 26.0 μM FeSO_4 , 23.8 μM NaEDTA , 3.5 μM MnCl_2 , 9.9 μM H_3BO_3 , 0.9 μM ZnSO_4 , 0.2 μM
126 CuSO_4 and 0.4 μM NaMoO_2 . In previous studies we noted an Al-induced decrease in gas
127 exchange rates when *C. limonia* was exposed to 1480 μM Al (40 mg L^{-1}) (Banhos et al., 2016;
128 Silva et al., 2018; Cavalheiro et al., 2020). Therefore, the solution contained the
129 aforementioned macro and micronutrients, as well as 0 and 1480 μM Al provided through
130 AlCl_3 . The nominal chemical composition of this solution was also tested on Geochem-EZ
131 software (Shaff et al., 2010), resulting in more than 85% free Al^{3+} available. The pH of the
132 solution was measured daily and maintained at 4.0 ± 0.1 (using NaOH and/or HCl) to guarantee
133 Al solubility. The solution was totally replaced every 15 days, and the treatment with no added
134 Al contained only trace amounts of Al.

135 Expanded polystyrene (Isopor®) 50 x 30 cm plates (2cm thick), with six holes (2.5 cm
136 in diameter) each, were floated on the nutrient solution in the boxes, and the plants were fixed
137 in these holes with polyurethane foam strips that were placed around the plant collar. The boxes
138 with six plants each were randomly arranged on benches (80 cm above the ground) inside a
139 greenhouse with semi-controlled conditions (air temperature $28.0 \pm 2^\circ\text{C}$; relative humidity 65.3
140 $\pm 2.5\%$ — between 9h and 11:30h). The photoperiod of 13h of natural sunlight measured inside
141 the greenhouse provided a photosynthetic photon flux density (PPFD) of 862.7 ± 184.4 μmol
142 $\text{photons m}^{-2} \text{s}^{-1}$, between 9h and 11:30h.

143

144 **2.2. Experimental design**

145 After transplant, six boxes (36 plants) remained with the nutrient solution containing 0
146 μM Al and six other boxes (36 plants) received the nutrient solution containing 1480 μM Al.
147 The plants grew in these conditions for 90 days, and non-destructive measurements (leaf gas
148 exchange) and destructive measurements (leaf water potential (Ψ_w), relative leaf water content
149 (RWC), NCED expression and ABA and its metabolites) were performed at 1, 7, 15, 30, 60
150 and 90 days after treatment (DAT). Using predawn (Ψ_{pd}) and midday (Ψ_{md}) leaf water potential
151 and transpiration rates measured in the afternoon, we also estimated the hydraulic conductivity
152 from roots to the leaves (K_L).

153 The excision of leaves for measuring Ψ_w , leaf discs for RWC and the collection of root
154 tips for gene expression analysis were not performed on the same plants used for measuring
155 leaf gas exchange, so that harmed plants did not interfere in the results of gas exchange rates.
156 Leaf discs for RWC and the collection of leaf pieces and root tips were performed within 60 s,
157 so that these variables interfered as little as possible in each other. In addition, the present study
158 did not involve repeated measurements on the same plants through time, as one box (with 6
159 plants) per treatment was used on each evaluation date. The leaf pieces and root tips were
160 collected, and their RNA was extracted for measuring NCED gene expression. Using six extra
161 plants (0 DAT and 90 DAT), the biomass of leaves, stems, roots and the total plant biomass
162 were assessed in order to check the severity of the Al treatment.

163

164 **2.3. Analysis**

165 **2.3.1. Leaf gas exchange**

166 CO_2 assimilation (A ; $\mu\text{mol m}^{-2} \text{s}^{-1}$) and transpiration (E ; $\text{mmol m}^{-2} \text{s}^{-1}$) rates, stomatal
167 conductance (g_s ; $\text{mol m}^{-2} \text{s}^{-1}$) and intercellular CO_2 (C_i ; $\mu\text{mol mol}^{-1}$) were measured using an
168 open gas exchange system (LI-6400xt; LI-COR, Lincoln, NE, USA). The water use efficiency
169 ($WUE = A/E$) and intrinsic water use efficiency ($iWUE = A/g_s$) were also calculated. The CO_2
170 concentration entering the leaf cuvette (LCF chamber; 2 cm^2 , LI-COR) averaged 400 μmol
171 mol^{-1} , as provided by the 6400-01 CO_2 mixer (LI-COR), as this was the air CO_2 concentration
172 accepted for the experimental site when the study was performed. Measurements were taken
173 between 9h and 11:30h on cloudless days, as it is the best period for measuring gas exchange
174 parameters (Feistler and Habermann, 2012). We also measured gas exchange in the afternoon
175 (13h-15h) in order to calculate the estimated hydraulic conductivity from roots to the leaves
176 (K_L).

177 The PPFD in the leaf cuvette was provided by an artificial LED light source (6400-40
178 LCF, LI-COR), which was set to provide 90% red and 10% blue light at 1500 $\mu\text{mol photons}$
179 $\text{m}^{-2} \text{s}^{-1}$, as this value saturates A for *C. limonia* as observed in A/C_i curves (Silva et al., 2018).
180 The vapor pressure deficit (VPD) inside the leaf cuvette was similar to the external
181 environment (inside the greenhouse), which was not higher than 1.5 kPa and relative humidity
182 was approximately 65% on the days of measurement.

183

184 2.3.2. Water relations

185 Ψ_{pd} and Ψ_{md} (under maximum VPD) were measured (MPa) by the pressure chamber method
186 (Turner, 1981), using a 3005F01 Plant Water Status Console (Soil Moisture, Santa Barbara,
187 CA, USA) chamber.

188 The estimated hydraulic conductivity from roots to the leaves (K_L ; $\text{mmol H}_2\text{O m}^{-2} \text{s}^{-1}$
189 MPa^{-1}) was determined by the method proposed by Hubbard et al. (2001), which is based on
190 Ohm's Law. For this, the following equation was applied:

$$191 K_L = E_{14\text{h}} / (\Psi_{\text{pd}} - \Psi_{\text{md}}),$$

192 where $E_{14\text{h}}$ is the transpiration rate (E) measured between 13:00h and 15:00h under maximum
193 VPD; Ψ_{pd} is assumed as the soil water potential (Ψ_{soil}), and Ψ_{md} is Ψ_w measured under
194 maximum VPD. Although the plants were grown directly on nutrient solution, the $\Psi_{\text{pd}} = \Psi_{\text{soil}}$
195 principle is still accepted because Ψ_{pd} is measured before sunrise in non-transpiring plants and,
196 therefore, Ψ_{pd} represents the plant's capacity to rehydrate overnight (Turner, 1981). This
197 method was previously used for measuring K_L in *Citrus sinensis* (Magalhães Filho et al., 2009)
198 and *C. limonia* (Cavalheiro et al., 2020) grown on nutrient solution.

199 For measuring RWC (%), leaf discs were collected at 13h-15h from plants of both
200 treatments and calculated as:

$$201 \text{RWC} = [(\text{FM} - \text{DM}) / (\text{TM} - \text{DM})] \times 100,$$

202 where FM is the fresh mass (immediately measured after collection); TM is the turgid mass,
203 measured after rehydrating samples for 24 h in 100 mL deionized water inside amber flasks
204 (to avoid photosynthetic activity); and DM is the dry mass, measured after oven-drying the
205 discs at 60°C for 48 h, according to Silva et al. (2018).

206

207 2.3.3. Gene expression analysis

208 Leaf pieces ($\approx 1 \text{ cm}^2$) or root pieces (1 cm in length), totaling 100 mg (fresh mass) for
209 each leaf or root sample ($n = 4$), were collected at 13h-15h, frozen in liquid nitrogen and stored

210 at -80°C for future analysis. Total RNA was extracted from leaf and root samples using the
211 RNeasy Plant Mini Kit (Qiagen, Hilden, Germany). Total RNA (2 µg) was treated with RNase-
212 free TURBO DNase (Ambion, Carlsbad, USA) and reverse transcribed to cDNA using oligo-
213 dT and the GoScript Reverse Transcription System kit (Promega Corp., Madison, WI, USA),
214 according to the manufacturer's protocol (Life Technologies, Carlsbad, CA, USA). Gene
215 expression analysis was carried out by quantitative real-time PCR (qRT-PCR) with SYBR
216 green GoTaq q-PCR Master Mix (Promega Corp., USA), using Applied Biosystems
217 QuantStudio 3 (Life Technologies, Carlsbad, CA, USA). The primers of *CINCED1*, *CINCED3*
218 and *CINCED5* (Table 1) used in the experiment were previously used in *Citrus* species (Agusti
219 et al., 2007, Bassene et al., 2009), including *C. limonia* (Neves et al., 2013). As reference genes,
220 we used glyceraldehyde-3-phosphate dehydrogenase (*GAPC2*) and elongation factor 1-alpha
221 (*EFα*) (Table 1), which were proposed by Mafra et al. (2012) and used previously by Silva et
222 al. (2019). Amplification efficiencies were calculated for each primer using Miner software
223 (Zhao and Fernald, 2005).

224 For calculating the relative expression, Ct (cycle threshold) values of each sample,
225 which were determined by the average of three technical replicates, were converted into
226 relative quantities (RQ) according to Pfaffl (2001), using the following equation:

$$227 \quad RQ = E^{\Delta Ct},$$

228 where E is the primer efficiency, and ΔCt is the difference between control Ct value for the
229 evaluated gene and Ct value of the given sample. A normalization factor (NF) for each sample
230 was calculated by the geometric mean of the RQ values of *GAPC2* and *EFα*. Normalized-
231 relative quantity (NRQ) of each sample was calculated as the ratio of the sample RQ and the
232 appropriate NF. Individual fold change values were determined by dividing the sample NRQ
233 by mean values of NRQ that were obtained from the calibrator, i.e., root samples of plants not
234 exposed to AI. Following this, fold change in the control group always shows a mean value of
235 1. Four independent biological replicates (plant samples) were used to calculate mean for each
236 time point and treatment combination.

237

238 **2.3.4. Quantification of ABA and metabolites**

239 ABA and its metabolites, phaseic acid (PA), dihydrophaseic acid (DPA), (+)-7'-
240 hydroxy-ABA (7'-OH ABA) and ABA-β-D-glucosyl ester (ABA-GE) were analyzed via liquid
241 chromatography/tandem mass spectrophotometry (LC/MS-MS) on a SciexExionLC coupled
242 with a QTRAP 6500+ mass spectrophotometer, following the method proposed by Morris et
243 al. (2019).

244 Leaf and root samples (500 mg DM) were ground to a powder (in 2 mL micro-
245 centrifuge tubes containing two 5 mm acid-rinsed glass balls) in a Star-Beater (VWR) at 30
246 Hz for 2 min. The powdered material, ~20 mg for leaf samples and ~50 mg for roots, with 1
247 ng of internal standards added, were extracted using a Star-Beater at 30 Hz for 2 min with 1
248 mL of ice-cold methanol/formic acid/water solvent (60:5:35 v/v). The internal standards used
249 were: [²H₄]-abscisic acid (-)-5,8',8',8' (d₄-ABA); [²H₃]-phaseic acid (-)-7',7',7' (d₃-PA); [²H₅]-
250 abscisic acid glucose ester (+)-4,5,8',8',8' (d₅-ABA-GE); [²H₃]-dihydrophaseic acid (-)-7',7',7'
251 (d₃-DPA); and [²H₄]-7'-hydroxy-abscisic acid (±)-5,8',8',8' (d₄-7OH-ABA). After extraction,
252 the samples were left on ice in the dark for 20 min and, subsequently, the plant material was
253 pelleted by centrifugation at 24,000 × g at 4°C for 10 min. The supernatant was pipetted into
254 15 mL conical centrifuge tubes and the solvent was evaporated overnight in a freeze-drier (-
255 105°C; Scanvac, CoolSafe 110-4 Pro). Samples were reconstituted (vortexed for 2 min at 1400
256 rpm, sonicated for 30s and a final vortex at 2000 rpm for 3 min) in 1 mL of 5% acetonitrile in
257 10 mM ammonium formate (pH 3.4, adjusted with formic acid). Finally, the samples were
258 filtered through 4 mm nylon filters (0.2 μM pore size, Whatman) into silanised amber HPLC
259 vials.

260 Calibration samples consisted of a series of non-deuterated compounds (from 0.1 to
261 500 ng mL⁻¹), each with deuterated compounds (constant 1 ng mL⁻¹). Extracts and calibration
262 samples (20 μL) were injected with an auto-sampler into a Luna 3 μm C18(2) 100 x 2 mm
263 (Phenomenex) column with guard column at 30°C. The aqueous mobile phase (A) consisted
264 of 2% acetonitrile in 10 mM ammonium formate, and the organic mobile phase (B) was 95%
265 acetonitrile and 0.1% formic acid. The ratios of mobile phase A:B for separation of compounds
266 was as follows (at a flow rate of 600 μL min⁻¹): 0-1.5 min at 96:4; 1.5-7 min at 87.4:12.6 and
267 7-10 min at 74:26. The column was then cleaned as follows, 10-10.5 min at 60:40; 10.5-10.6
268 min at 50:50 and 10.6-11.6 min at 0:100. The column was then equilibrated from 11.6-13 min
269 at 96:4 before injection of the next sample. Analyst 1.6.3 and MultiQuant 3.0.2 (Sciex,
270 Singapore) software was used for acquisition and quantification, respectively.

271

272 **2.3.5. Biometric parameters**

273 At 0 and 90 DAT, after separating the plant parts into leaves (plus petioles), stems and
274 roots, the number of leaves was counted, and the shoot length was measured with a ruler. The
275 total leaf area per plant (LA) was measured with an area meter (LI-3100C, LI-COR, USA).
276 Total root length, root surface area and root diameter were measured using a scanner (Epson
277 perfection v700 photo, Suwa, Japan), which was coupled to a computer running the

278 WinRHIZO™ software (Regent Instruments, Canada). The biomass of organs was measured
279 on a 0.001g precision scale (AR2140, OHAUS, USA) after oven-drying the samples at 60°C
280 until constant mass.

281

282 **2.3.6. Aluminum quantification**

283 Dry samples of leaves and roots were sent to a plant nutrition laboratory at University
284 of São Paulo (ESALQ, USP, Piracicaba, Brazil) where these were ground and digested in a
285 solution of sulfuric:nitric:perchloric acids (1:10:2, v/v/v). After digestion, Al concentrations
286 were determined by the atomic absorption spectrophotometer method (Sarruge and Haag,
287 1974) and expressed as mg Al per kg dry mass.

288

289 **2.3.7. Data analysis**

290 Leaf gas exchange parameters (A , g_s , E , C_i , WUE and $iWUE$), RWC and biomass of
291 organs were measured using six plant replicates. Leaf water potential (Ψ_{pd} and Ψ_{md}), estimation
292 of hydraulic conductivity from roots to the leaves (K_L), gene expression of NCED and ABA
293 metabolites were assessed using four plant replicates.

294 A student's t-test ($\alpha = 0.05$) was used, separately for each evaluation date (1, 7, 15, 30,
295 60 and 90 DAT), to test differences between 0 and 1480 μM Al for each variable, as well as
296 when testing differences in plant biomass and Al concentration in plant organs between 0 and
297 90 DAT within each treatment.

298

299 **3. Results**

300 *3.1. Biometric parameters*

301 As expected, Al reduced the size of plants (Supplementary material; Fig. S1). At 90
302 DAT, Al significantly limited the main root length (-48%) (Fig. 1A), root surface area (-62%)
303 (Fig. 1B) and root biomass (-65%) (Fig. 1D), while the root diameter was enhanced in plants
304 exposed to Al (+25%) (Fig. 1C).

305 From 0 to 90 DAT, the leaf number (Fig. 2A), leaf area (Fig. 2B) and leaf biomass (Fig.
306 2C) increased by 31%, 83% and 59%, respectively, in plants exposed to Al and 140%, 504%
307 and 393%, respectively, in control plants. At 90 DAT, Al significantly decreased the leaf
308 number (-45%) (Fig. 2A), leaf area (-70%) (Fig. 2B) and leaf biomass (-68%) (Fig. 2C). Thus,
309 Al inhibited root growth, leaf initiation, leaf expansion and organ biomass accumulation, but
310 caused root thickening.

311

312 3.2. Leaf gas exchange

313 Compared to plants not exposed to Al, values of A (Fig. 3A), g_s (Fig. 3B) and E (Fig.
314 3C) decreased from 7 DAT, and at 90 DAT these parameters were 71%, 78% and 60% lower
315 in plants exposed to Al. On the other hand, C_i values increased in plants exposed to Al from
316 15 DAT, being 55% higher at 90 DAT (Fig. 3D). The WUE was the same between the
317 treatments throughout the study (Fig. 3E), while $iWUE$ was higher in plants exposed to Al from
318 30 DAT, being 108% higher at 90 DAT (Fig. 3F). This data is consistent with stomatal closure
319 leading to reductions of A . That is, a larger effect of Al toxicity on g_s than on A resulted in an
320 increase in A/g_s ($iWUE$).

321

322 3.4. Water relations

323 Ψ_{pd} was lower in plants exposed to Al throughout the study, although this was not
324 statistically significant (Fig. 4A). However, plants exposed to Al showed significantly lower
325 Ψ_{md} (Fig. 4B) and RWC (Fig. 5A) when compared to control plants from 7 DAT onwards. At
326 90 DAT, Al reduced Ψ_{md} from -1.2 to -2.2 (Fig. 4B) and RWC from 89% to 67% (Fig. 5A).
327 K_L was also lower in plants exposed to Al from 7 DAT, being 80% lower than control plants
328 at 90 DAT (Fig. 5B). Thus, Al compromised plant water status.

329

330 3.5. NCED gene expression

331 In the leaves, Al enhanced NCED genes expression over time (Fig. 6A, 6C and 6E),
332 while in the roots Al caused a peak for *CINCED5* (Fig. 6F) and *CINCED3* (Fig. 6D), most
333 pronounced in the latter. The Al-induced up-regulation of leaf *CINCED3* started at 15 DAT,
334 being 78-fold higher at 90 DAT (Fig. 6C). For leaf *CINCED1* and *CINCED5*, significant up-
335 regulation occurred at 60 and 90 DAT, and on these dates up-regulation was of approximately
336 80- (Fig. 6A) and 35-fold higher (Fig. 6E) than the control, respectively. In the roots, Al caused
337 up-regulation of *CINCED3* on all dates except for 7 DAT, reaching a peak of 16-fold higher
338 than control plants at 30 DAT (Fig. 6D). Root *CINCED5* was significantly up-regulated by Al
339 (4-fold higher) only at 60 DAT, while no up-regulation in root *CINCED1* was induced by Al
340 (Fig. 6B). Thus, Al up-regulated the key genes of ABA biosynthesis (*CINCED3*) in the roots
341 at 1 DAT (Fig. 6D), while decreases in leaf hydration were detected at 7 DAT for g_s (Fig. 3B),
342 Ψ_{md} (Fig. 4B), RWC (Fig. 5A) and K_L (Fig. 5B).

343

344 3.6. Abscisic acid (ABA) accumulation in leaves and roots

345 In general, Al increased ABA concentrations in leaves and roots (Fig. 7A, 7B). In plants
346 exposed to Al, [ABA]_{leaf} increased from 7 DAT, being 4.7-times higher than the control at 90
347 DAT (Fig. 7A). [DPA]_{leaf} and [7'OH ABA]_{leaf} increased in plants exposed to Al from 15 DAT,
348 being 1.3- and 1.5-times higher than the control, respectively, over this period (Fig. 7E, 7G).
349 [PA]_{leaf} and [ABA-GE]_{leaf}, however, were higher in plants exposed to Al only at 90 DAT, being
350 2.6- and 2.0-times higher, respectively, when compared to the control (7C, 7I). Therefore, Al
351 caused a consistent increase in [ABA], [DPA] and [7'OH ABA] from the first week of the
352 study, while [PA] and [ABA-GE] increased only after 90 days of Al exposure.

353 In the roots, Al caused a peak of [ABA]_{root} (3-times higher than the control; Fig. 7B),
354 [PA]_{root} (7-times higher; Fig. 7D) and [ABA-GE]_{root} (3.3-times higher; Fig. 7J) at 7, 1 and 30
355 DAT, respectively. After these peaks, the concentration of these metabolites in the roots
356 decreased, but remained higher in plants exposed to Al at 15 and 30 DAT (ABA; Fig. 7B), 30
357 and 60 DAT (PA; Fig. 7D) and until 90 DAT (ABA-GE; Fig. 7J). [DPA]_{root} of plants exposed
358 to Al was 2.0-times higher than control plants only at 90 DAT (Fig. 7F), while [7'OH ABA]_{root}
359 showed no pattern, with variable values between treatments (Fig. 7H).

360 Thus, Al increased ABA in the roots immediately after Al exposure and, in the leaves,
361 Al induced a consistent accumulation, especially for ABA, DPA and 7'OH ABA. In the leaves
362 of plants exposed to Al, ABA accumulation seems to be associated with *CINCED3*
363 (Supplementary material; Fig. S2). In addition, in Al-treated plants, [ABA]_{leaf} is driving major
364 part of g_s responses (Supplementary material; Fig. S3), which also corroborates low values of
365 RWC, Ψ_{md} and K_L of plants exposed to Al.

366

367 3.7. Aluminum retention in plant organs

368 As expected, Al concentration in the roots was approximately 10 times higher than the
369 leaves of plants exposed to Al (Fig. 8). From 0 to 90 DAT, leaf and root Al concentration
370 increased by seven- (Fig. 8A) and 15-times (Fig. 8B), respectively, in control plants when
371 compared to those treated with Al.

372

373 4. Discussion

374 Hydraulic signals, in the form of turgor changes in the leaves, and hormonal signaling
375 have been proposed to control g_s (McAdam and Brodribb, 2015; Huber et al., 2019). Plant
376 hormones can influence the Al toxicity and development of symptoms (Kopittke, 2016), as
377 well as these compounds can mediate the Al resistance, especially in the root environment

378 (Massot et al., 2002; Yang et al., 2017). The well-known role of ABA in causing stomatal
379 closure, the up regulation of ABA biosynthesis upon changes in cell turgor and water
380 availability (McAdam et al., 2016; Susmilch et al., 2017; Zhang et al., 2018) makes ABA a
381 candidate for causing the decrease in g_s during Al toxicity. In the present study, we tested
382 whether ABA accumulation in roots and leaves could be responsible for the Al-induced low g_s
383 usually found in *Citrus limonia* exposed to Al (Banhos et al., 2016; Silva et al., 2018;
384 Cavalheiro et al., 2020).

385

386 4.1. Effect of Al on plant water relations

387 Our results show that A and E were progressively reduced in plants exposed to Al (Fig.
388 3A and 3C), and these reductions could be explained by the low g_s values (Fig. 3B). In our
389 previous studies with this same species under the same Al concentration, low A values were
390 largely explained by low g_s rather than decreased photochemical performance (Banhos et al.,
391 2016; Silva et al., 2018). In addition, Al-induced reduction in g_s has been observed in other
392 *Citrus* plants, including ‘Cleopatra’ tangerine (-30%; Chen et al., 2005b) and ‘Sour Pummelo’
393 (-40%; Jiang et al., 2008). Therefore, the decrease in g_s seems to be a key response in plants
394 exposed to Al.

395 Plants adjust their xylem pressure with concomitant stomatal regulation (Creek et al.,
396 2020; Rodriguez-Dominguez and Brodribb, 2019). In the present study, the decrease in g_s of
397 plants exposed to Al was not sufficient to maintain the leaf water status, as evidenced by low
398 values of Ψ_{md} (Fig. 4B) and RWC (Fig. 5A) from 7 DAT. K_L represents the plant capacity to
399 supply water to the mesophyll (Rodríguez-Gamir et al., 2019) and since its value dropped by
400 80% under Al toxicity (Fig. 5B), the ability of the Al-treated plants to transport water to the
401 leaves was dramatically impaired. Indeed, root hydraulic conductance (Lp_r) of *Solanum*
402 *lycopersicum* (tomato) also declined proportionally to the increase of Al in nutrient solution
403 (Gavassi et al., 2020). Reductions in K_L and low expression of aquaporins (PIP family) in *C.*
404 *limonia* exposed to 1480 μ M Al found by Cavalheiro et al. (2020) have been associated with
405 fibrous xylem vessels (Banhos et al., 2016) and more lignin deposition in the vascular cylinder
406 (Silva et al., 2019) of *C. limonia* grown under the same Al toxicity conditions. The root apex
407 senses Al toxicity (Ryan et al., 1993; Horst et al., 2010), and, despite being anatomically
408 “disconnected” from the xylem, the longer the exposure of root tips of *C. limonia* to Al, the
409 more lignin deposition is found in their vascular cylinders (Silva et al., 2019), although the
410 mechanism(s) of signaling between Al perception and xylem damage is unclear. The vascular
411 cylinder was also the most affected part of the root of maize plants, and their proto- and

412 metaxylem did not reach full maturation under 300 μM Al (Batista et al., 2013). In addition,
413 ten-times more Al was found in root tips (1 cm long) of maize plants exposed to 50 μM Al
414 when compared to plants not exposed to Al after 24h (Souza et al., 2016). This same proportion
415 was found in the roots of plants exposed to Al when compared to control plants, at 90 DAT
416 (Fig. 8B). Furthermore, once Al is firmly bound to a root cell wall, where it is the site of
417 primary lesion (Kopittke et al., 2015), it does not seem to be released (Rangel et al., 2009), and
418 it could cause anatomical damage to the cortex and xylem of plant roots, as observed by Batista
419 et al. (2013), Banhos et al. (2016) and Silva et al. (2019). Taken together, these results suggest
420 that Al impairs the plant capacity to transport water to the leaves. A key question, however, is
421 whether the impairment of root and vascular function leads directly to declining shoot water
422 status and productivity (reduced g_s , A and biomass), or whether this is controlled by early
423 hormonal signals.

424

425 4.2. The role of ABA and its metabolites in short-term responses

426 In the present study, root ABA increased at 1 DAT (Fig. 7B) relative to control, prior
427 to any significant decreases in Ψ_{pd} , Ψ_{md} , RWC or K_L (Fig. 4 and 5); and ABA kept increasing
428 in the root until 7 DAT (Fig. 7B). PA concentration was also higher at 1 DAT, compared to
429 control plants (Fig. 7D); this could also contribute to physiological responses because PA
430 showed biological activity *in vitro*, activating members of the ABA receptor family, albeit with
431 a lower affinity than ABA (Weng et al. 2016). Although not presenting biological activity,
432 ABA-GE was higher in the roots of plants exposed to Al on all dates, including 1 DAT,
433 although showing a peak at 30 DAT (Fig 7J). ABA-GE is considered an ABA metabolite and
434 can be transported symplastically from the cytosol of root cells to xylem parenchyma cells and
435 be released to xylem vessels (Priest et al., 2006) as a root-to-shoot signal (Sauter et al., 2002).
436 Therefore, the extra ABA-GE produced from 1 DAT in the Al-treated roots could have been
437 transported, de-glycosylated and have contributed to the ABA level and stomatal closure at 7
438 DAT. Analysis of gene expression in the early period 1-7 DAT indicated that *CINCED3*
439 responded to the Al treatment in the roots, but the increase was small (Fig. 6D). This small
440 increase could have contributed to the rise in ABA, PA and ABA-GE. Alternatively, an
441 activation of NCED enzyme activity at the protein level, or a change in transport processes
442 between root and shoot might explain the early spike in ABA given that there was only a small
443 increase in *CINCED3* gene expression. Furthermore, the catabolic product PA increased at 1

444 DAT (Fig. 7D), suggesting that slower ABA catabolism was not the reason for ABA
445 accumulation in the roots of Al-treated plants.

446 Overall, the very early rise in root ABA, PA and ABA-GE caused by Al toxicity
447 appeared to precede the decline in g_s , and so is potentially the cause of stomatal closure.
448 However, this reduction in g_s , preventing water loss, was not able to stop a decline in leaf water
449 status, presumably caused by the impact of Al on root water transport function as suggested by
450 Batista et al. (2013), Banhos et al. (2016), Silva et al. (2019), Cavaleiro et al. (2020) and
451 Gavassi et al. (2020), and also supported by the 80% lower K_L in plants exposed to Al (Fig.
452 5B). The coincident reduction in g_s and shoot water status at 7 DAT means that we cannot
453 exclude a hydraulic signal as the cause of stomatal closure.

454

455 4.3. The role of ABA and metabolites in longer-term responses

456 In the leaves of plants exposed to Al, ABA progressively increased until the end of the
457 study (Fig. 7A) with the first significant increase occurring at 7 DAT. This was accompanied
458 by similar trends of DPA from 15 DAT (Fig. 7E), but surprisingly $[DPA]_{\text{leaf}}$ peaked 25-fold
459 higher in absolute concentration than $[ABA]_{\text{leaf}}$, suggesting a high rate of catabolism to DPA
460 that has previously been observed in *Citrus* leaves under drought and soil flooding stresses
461 (Jitratham et al., 2006; Arbona et al., 2017). ABA accumulation in the leaf occurred later and
462 more progressively than in the root, and after, or co-incident with, the decline in water relations
463 (RWC, Ψ_{md} and K_L all down at 7 DAT). Therefore the leaf ABA and PA was likely increased as
464 a secondary consequence of the Al toxicity, where lack of water supply to the shoot (low K_L)
465 led to reduced shoot water status which then stimulated accumulation of ABA and PA and
466 reinforced stomatal closure: in plants exposed to Al, $[ABA]_{\text{leaf}}$ was inversely correlated with
467 g_s values (Supplementary material; Fig. S3).

468 The expression of genes encoding NCED did not fully explain the increase in ABA and
469 DPA in the leaf. The first increase was for *CINCED3* at 15 DAT, after the rise in ABA, and
470 this initial increase for *CINCED3* was small (2-fold), with the peak occurring at 90 DAT (Fig.
471 6C). However, the linear correlation (R^2) between *CINCED3* and $[ABA]_{\text{leaf}}$ in plants exposed
472 to Al was 0.875 (Supplementary material; Fig. S2). This suggests that progressive increase in
473 $[ABA]_{\text{leaf}}$ may be explained by *CINCED3* expression. In the leaf, *CINCED1* and *CINCED5*
474 also showed up-regulation of approximately 80- and 30-fold higher than control plants,
475 respectively, at 60 and 90 DAT (Fig. 6A and 6E), but this rise was even later than for
476 *CINCED3*; therefore it did not explain the initial increase in ABA from 7 DAT in the leaf, but
477 may have contributed to the continued and accelerated increase in ABA and PA which showed

478 a sharp rise between 60 and 90 DAT. The increase in *CINCED3* expression from 15 DAT, and
479 of *CINCED1* and *CINCED5* from 60 DAT, was probably driven by reduced cellular water
480 status in the leaf since orthologs of this gene are known to respond in this way. In *Arabidopsis*,
481 the orthologous *AtNCED3* is predominantly induced by drought and controls endogenous ABA
482 content in this condition (Endo et al., 2008; Hao et al., 2009), but *AtNCED5* and *AtNCED3*
483 participate together in water deficit response (Frey et al., 2012). In *Citrus*, *NCED1* was up-
484 regulated by drought in leaves of *C. sinensis* (Rodrigo et al., 2006; Xian et al., 2014) and *C.*
485 *resnyi* (Zandalinas et al., 2016), as also observed here in the leaves of plants exposed to Al
486 (Fig. 6A). Up-regulation of *CINCED5* was previously observed in leaves of *C. limonia*
487 submitted to 40 days of drought (Neves et al., 2013).

488 Thus, only the later, but not the early increase in ABA and DPA, could be explained by
489 *NCED* gene expression in the leaves; other mechanisms, such as reduced catabolism, post-
490 transcriptional control or redistribution of ABA would need to be invoked.

491

492 4.4. Impact of reduced growth rate on physiological responses

493 Critics could still argue that the conspicuous decrease in root growth parameters caused
494 by Al at 90 DAT (Fig. 1A, 1B and 1D) could have acted as a physical limitation for water
495 uptake, which could not maintain leaf transpiration, explaining the low g_s values. However,
496 this low root growth was followed by reduced leaf number (Fig. 2A), leaf area (Fig. 2B) and
497 leaf biomass (Fig. 2C), which would have greatly reduced the demand for water transport from
498 the smaller root system. Similarly, tomato plants exposed to 0, 25 and 50 μM Al showed similar
499 root/leaf area ratio, reinforcing that the decrease in the root size is compensated by a low shoot
500 growth (Gavassi et al., 2020).

501 We have measured biometric parameters only at 90 DAT, but it seems unlikely that
502 reduced root growth could have occurred at 7 DAT and have caused low g_s values due to fewer
503 roots responsible for (less) water uptake. Further evidence in this regard deserves investigation.

504

505 5. Conclusions

506 We showed that Al triggered *CINCED3* expression and ABA biosynthesis in the roots
507 1 day after Al exposure in *C. limonia*, before impairments in leaf hydration (low Ψ_w , RWC
508 and g_s) could be observed. In addition, leaf ABA concentration increased from 7 to 90 DAT
509 and this could be partially explained by the increased expression of *CINCED3*, *CINCED1* and
510 *CINCED5* in this organ. Stomatal closure occurred concomitantly with the increase of ABA

511 concentration and this result provides further evidence of the role of ABA modulation of plant
512 hydration under AI stress.

513

514 **Acknowledgements**

515 We thank the Sanicitrus Nursery (Araras, São Paulo state, Brazil) for providing us with
516 the *C. limonia* plants.

517

518 **Funding sources**

519 This work was supported by the São Paulo Research Foundation (Fapesp) [grant
520 numbers 2015/25409-4, 2018/08902-7, 2018/25658-2, 2017/26144-0] and the Brazilian
521 National Council for Scientific and Technological Development (CNPq) [grant number
522 141342/2016-1, 309149/2017-7].

523

524

525

526

References

- Agusti, J., Zapater, M., Iglesias, D.J., Cercós, M., Tadeo, F.R., Talón, M., 2007. Differential expression of putative 9-cis epoxy-carotenoid dioxygenases and abscisic acid accumulation in water stressed vegetative and reproductive tissues of citrus. *Plant Sci.* 172, 85–94.
- Ali, S., Zeng, F., Qiu, L., Zhang, G. 2011. The effect of chromium and aluminum on growth, root morphology, photosynthetic parameters and transpiration of the two barley cultivars. *Biol. Plant.* 55, 291-296.
- Anjum, A.S., Ashraf, U., Khan, I., Tanveer, M., Saleem, M.F., Wang, L. 2016. Aluminum and chromium toxicity in maize: implications for agronomic attributes, net photosynthesis, physio-biochemical oscillations, and metal accumulation in different plant parts. *Water Air Soil Pollut.* 227, 326.
- Arbona, V., Zandalinas, S.I., Manzi, M., González-Guzmán, M., Rodríguez, P.L., Gómez-Cadenas, A., 2017. Depletion of abscisic acid levels in roots of flooded Carrizo citrange (*Poncirus trifoliata* L. Raf. × *Citrus sinensis* L. Osb.) plants is a stress-specific response associated to the differential expression of PYR/PYL/RCAR receptors. *Plant Mol. Biol.* 93, 623-640.
- Banhos, O.F.A.A., Carvalho, B.M.O., Veiga, E.B., Bressan, A.C.G., Tanaka, F.A.O., Habermann, G., 2016. Aluminum-induced decrease in CO₂ assimilation in ‘Rangpur’ lime is associated with low stomatal conductance rather than low photochemical performances. *Sci. Hortic.* 205, 133-140.
- Bassene, J.B., Froelicher, Y., Dhuique-Mayer, C.M., Mouhaya, W., Ferrer, R.M., Ancillo, G., Morillon, R., Navarro, L., Ollitraut, P., 2009. Nonadditive phenotypic and transcriptomic inheritance in a citrus allotetraploid somatic hybrid between *C. reticulata* and *C. limon*: the case of pulp carotenoid biosynthesis pathway. *Plant Cell Rep.* 28, 1689–1697.
- Batista, M.F., Moscheta, I.S., Bonato, C.M., Batista, M.A., Almeida, O.J.G., Inoue, T.T., 2013. Aluminum in corn plants: influence on growth and morpho-anatomy of root and leaf. *Rev Bras Cienc Solo* 37, 177-187.
- Cavalheiro, M.F., Gavassi, M.A., Silva, G.S., Nogueira, M.A., Silva, C.M.S., Domingues, D.S., Habermann, G., 2020. Low root PIP1-1 and PIP2 aquaporins expression could be related to reduced hydration in ‘Rangpur’ lime plants exposed to aluminum. *Funct. Plant Biol.* 47, 112-121.
- Clark, R.B., 1975. Characterization of phosphatase of intact maize roots. *J. Agric. Food Chem.* 23, 458–460.
- Chen, L-S., Qi, Y.-P., Smith, B.R., Liu, X.H., 2005. Aluminum-induced decrease in CO₂ assimilation in citrus seedlings is unaccompanied by decreased activities of key enzymes involved in CO₂ assimilation. *Tree Physiol.* 25, 317–324.
- Creek, D., Lamarque, L.J., Torres-Ruiz, J.M., Parise, C., Burlett, R., Tissue, D.T., Delzon, S., 2020. Xylem embolism in leaves does not occur with open stomata: evidence from direct observations using the optical visualization technique. *J. Exp. Bot.* 71, 1151-1159.
- Cutler, A.J., Krochko, J.E., 1999. Formation and breakdown of ABA. *Trends Plant Sci.* 4, 472–478
- Dodd, I.C., 2003. Leaf area development of ABA-deficient and wildtype peas at two levels of nitrogen supply. *Funct. Plant Biol.* 30, 777–783.

- Endo, A., Sawada, Y., Takahashi, H., Okamoto, M., Ikegami, K., Koiwai, H., Seo, M., Toyomasu, T., Mitsuhashi, W., Shinozaki, K., Nakazono, M., Kamiya, Y., Koshihara, T., Nambara, E., 2008. Drought induction of Arabidopsis 9-cis-epoxycarotenoid dioxygenase occurs in vascular parenchyma cells. *Plant Physiol.* 147, 1984–1993.
- Estrada-Melo, A.C., Reid, M.S., Jiang, C.Z., 2015. Overexpression of an ABA biosynthesis gene using a stress-inducible promoter enhances drought resistance in petunia. *Hort. Res.* 2, 15013.
- Feistler, A.M., Habermann, G., 2012. Assessing the role of vertical leaves within the photosynthetic function of *Styax camporum* under drought conditions. *Photosynthetica* 50, 613–622.
- Frey, A., Effroy, D., Lefebvre, V., Seo, M., Perreau, F., Berger, A., Sechet, J., To, A., North, H.M., Marion-Poll, A., 2012. Epoxycarotenoid cleavage by NCED5 fine-tunes ABA accumulation and affects seed dormancy and drought tolerance with other NCED family members. *Plant J* 70, 501–512.
- Gavassi, M.A., Dodd, I.C., Puértolas, J., Silva, G.S., Carvalho, R.F., Habermann, G., 2020. Aluminum-induced stomatal closure is related to low root hydraulic conductance and high ABA accumulation. *Env. Exp. Bot. in press.* doi: <https://doi.org/10.1016/j.envexpbot.2020.104233>
- Gunsé, B., Poschenrieder, C., Barceló, J., 1997. Water transport properties of roots and root cortical cells in proton- and Al-stressed maize varieties. *Plant Physiol.* 113, 595–602.
- Hao, G.P., Zhang, X.H., Wang, Y.Q., Wu, Z.Y., Huang, C.L., 2009. Nucleotide variation in the NCED3 region of *Arabidopsis thaliana* and its association study with abscisic acid content under drought stress. *J Integr Plant Biol* 51, 175–183.
- Horst, W.J., Wang, Y., Eticha, D. 2010. The role of the root apoplast in aluminium-induced inhibition of root elongation and in aluminium resistance of plants: a review. *Ann. Bot.* 106, 187–197.
- Hou, N., You, J., Pang, J., Xu, M., Chen, G., Yang, Z., 2010. The accumulation and transport of abscisic acid in soybean (*Glycine max* L.) under aluminum stress. *Plant Soil* 330, 127–137.
- Hubbard, R.M., Ryan, M.G., Stiller, V., Sperry, J.S. 2001. Stomatal conductance and photosynthesis vary linearly with plant hydraulic conductance in ponderosa pine. *Plant Cell Environ.* 24, 113–121.
- Huber, A.E., Melcher, P.J., Piñeros, M.A., Setter, T.L., Baueler, T.L., 2019. Signal coordination before, during and after stomatal closure in response to drought stress. *New Phytol.* 224, 675–688.
- Iuchi, S., Kobayashi, M., Taji, T., Naramoto, M., Seki, M., Kato, T., Tabata, S., Kakubari, Y., Yamaguchi-Shinozaki, K., Shinozaki, K., 2001. Regulation of drought tolerance by gene manipulation of 9-cisepoxycarotenoid dioxygenase, a key enzyme in abscisic acid biosynthesis in Arabidopsis. *Plant J.* 27, 325–333.
- Jiang, H-X., Chen, L-S., Zheng, J-G., Han, S., Tang, N., Smith, B.R., 2008. Aluminum-induced effects on Photosystem II photochemistry in Citrus leaves assessed by the chlorophyll a fluorescence transient. *Tree Physiol.* 28, 1863–1871.
- Jitratham, A., Yazama, F., Kondo, S., 2006. Effects of drought stress on abscisic acid and jasmonate metabolism in *Citrus*. *Environ. Control Biol.* 44, 41–49.
- Kopittke, P.M., Blamey, F.P.C., Menzies, N.W., 2008. Toxicities of Al, Cu, and La include ruptures to rhizodermal and root cortical cells of cowpea. *Plant Soil* 303, 217–227.
- Kopittke, P.M., Moore, K.L., Lombi, E., Gianoncelli, A., Ferguson, B.J., Blamey, F.P.C., Menzies, N.W., Nicholson, T.M., McKenna, B.A., Wang, P., Gresshoff, P.M., Kourousias, G., Webb, R.I.,

- Green, K., Tollenaere, A., 2015. Identification of the primary lesion of toxic aluminum in plant roots. *Plant Physiol.* 167, 1402-1411.
- Kopittke, P.M., 2016. Role of phytohormones in aluminium rhizotoxicity. *Plant Cell Environ.* 39, 2319-2328.
- Ma, Y., Cao, J., He, J., Chen, Q., Li, X., Yang, Y., 2018. Molecular Mechanism for the Regulation of ABA Homeostasis During Plant Development and Stress Responses. *Int. J. Mol. Sci.* 19, 3643.
- Mafra, V., Kubo, K.S., Alves-Ferreira, M., Ribeiro-Alves, M., Stuart, R.M., Boava, L.P., Rodrigues, C.M., Machado, M.A., 2012. Reference genes for accurate transcript normalization in citrus genotypes under different experimental conditions. *PLoS ONE* 7, e31263.
- Magalhães Filho, J.R., Machado, E.C., Machado, D.F.S.P., Ramos, R.A., Ribeiro, R.V., 2009. Variação da temperatura do substrato e fotossíntese em mudas de laranjeira 'Valência'. *Pesq. Agropec. Bras.* 44, 1118–1126.
- Massot, N., Nicander, B., Barceló, J., Poschenrieder, C., Tillberg, E., 2002. A rapid increase in cytokinin levels and enhanced ethylene evolution precede Al³⁺-induced inhibition of root growth in bean seedlings (*Phaseolus vulgaris* L.). *Plant Growth Regul.* 37, 105–112.
- McAdam, S.A.M., Brodribb T.J., 2015. The evolution of mechanisms driving the stomatal response to vapor pressure deficit. *Plant Physiol.* 167, 833–843.
- McAdam, S.A.M., Sussmilch, F.C., Brodribb, T.J., 2016. Stomatal responses to vapour pressure deficit are regulated by high speed gene expression in angiosperms. *Plant Cell Environ.* 39, 485–491.
- Merilo, E., Jalakas, P., Laanemets, K., Mohammadi, O., Hōrak, H., Kollist, H., Brosche, M., 2015. Abscisic acid transport and homeostasis in the context of stomatal regulation. *Mol. Plant* 8, 1321-1333.
- Mehrotra, R., Bhalothia, P., Bansal, P., Basantani, M.K., Bharti., V., Mehrotra S., 2014. Abscisic acid and abiotic stress tolerance – Different tiers of regulation. *Plant Physiol.* 171, 486-496.
- Morris, W.L., Alamar, M.C., Lopez-Cobollo, R.M., Castillo, J.C., Bennett, M., Van der Kaay, J., Stevens, J., Sharma, S.K., McLean, K., Thompson, M.J., Terry, L.A., Turnbull, C.G.N., Bryan, G.J., Taylor, MA., 2019. A member of the TERMINAL FLOWER 1/CENTRORADIALIS gene family controls sprout growth in potato tubers. *J. Exp. Bot.* 70, 835–843.
- Neves, D.M., Coelho Filho, M.A., Bellete, B.S., Silva, M.F.G.F., Souza, D.T., Soares Filho, W.S., Costa, M.G.C., Gesteira, A.S., 2013. Comparative study of putative 9-cis-epoxycarotenoid dioxygenase and abscisic acid accumulation in the responses of Sunki mandarin and Rangpur lime to water deficit. *Mol. Biol. Rep.* 40, 5339–5349.
- Ng, L.M., Melcher, K., The, B.T., Xu, H.E., 2014. Abscisic acid perception and signaling: structural mechanisms and applications. *Acta Pharm. Sin.* 35, 567–584.
- Okamoto, M., Tanaka Y., Abrams S.R., Kamiya Y., Seki M., Nambara E., 2009. High humidity induces abscisic acid 8'-hydroxylase in stomata and vasculature to regulate local and systemic abscisic acid responses in *Arabidopsis*. *Plant Physiol.* 149, 825–834.
- Panda, S.K., Baluska, F., Matsumoto, H., 2009. Aluminum stress signaling in plants. *Plant Signal. Behav.* 4, 592-597.
- Pfaffl, M.W., 2001. A new mathematical model for relative quantification in real-time RT PCR. *Nucleic*

Acids Res. 29, 45–45.

Priest, D.M., Ambrose, S.J., Vaistij, F.E., Elias, L., Higgins, G.S., Ross, A.R., Abrams, S.R., Bowles, D.J., 2006. Use of the glucosyltransferase UGT71B6 to disturb abscisic acid homeostasis in *Arabidopsis thaliana*. *Plant J.* 46, 492–502.

Rangel, A.F., Rao, I.M., Horst, W.J., 2009. Intracellular distributing and bidding state of aluminum in root apices of two common bean (*Phaseolus vulgaris*) genotypes in relation to Al toxicity. *Physiol. Plant.* 135, 162–173.

Reyna-Llorens, I., Corrales, I., Poschenrieder, C., Barcelo, J., Cruz-Ortega, R., 2015. Both aluminum and ABA induce the expression of an ABC-like transporter gene (FeALS3) in the Al-tolerant species *Fagopyrum esculentum*. *Env. Exp. Bot.* 111, 74–82.

Rodrigo, M.J., Alquezar, B., Zacarías L., 2006. Cloning and characterization of two 9-*cis*-epoxycarotenoid dioxygenase genes, differentially regulated during fruit maturation and under stress conditions, from orange (*Citrus sinensis* L. Osbeck). *J. Exp. Bot.* 57, 633–643.

Rodriguez-Dominguez, C.M., Brodribb, T.J., 2019. Declining root water transport drives stomatal closure in olive under moderate water stress. *New Phytol.* 225, 126-134.

Rodríguez-Gamir, J., Xue, J., Clearwater, M.J., Meason, D.F., Clinton, P.W., Domec, J-C., 2019. Aquaporin regulation in roots controls plant hydraulic conductance, stomatal conductance, and leaf water potential in *Pinus radiata* under water stress. *Plant Cell Environ.* 42, 717-729.

Ryan, P.R., Ditomaso, J.M., Kochian, L.V., 1993. Aluminium toxicity in roots: an investigation of spatial sensitivity and the role of the root cap. *J Exp Bot.* 44, 437–446.

Sarruge, J.R., Haag, H.P., 1974. Análises químicas em plantas. Piracicaba, ESALQ.

Sauter, A., Dietz K.-J., Hartung, W., 2002. A possible stress physiological role of abscisic acid conjugates in root-to-shoot signalling. *Plant Cell Environ.* 25, 223–228.

Shaff, J.E., Shultz, B.A., Craft, E.J., Clark, R.T., Kochian, L.V., 2010. GEOCHEM-EZ: A chemical speciation program with greater power and flexibility. *Plant Soil* 330, 207–214.

Shen, H., Ligaba, A., Yamaguchi, M., Osawa, H., Shibata, K., Yan, X., Matsumoto H., 2004. Effect of K-252a and abscisic acid on the efflux of citrate from soybean roots. *J Exp Bot.* 55, 663-671.

Silva, S., Pinto, G., Dias, M.C., Correira, C.M., Moutinho-Pereira, J., Pinto-Carnide, O., Santos, C., 2012. Aluminum long-term stress differently affects photosynthesis in rye genotypes. *Plant Physiol. Biochem.* 54, 105-112.

Silva, G.S., Gavassi, M.A., Nogueira, M.A., Habermann, G., 2018. Aluminum prevents stomatal conductance from responding to vapor pressure deficit in *Citrus limonia*. *Environ. Exp. Bot.* 155, 662–671.

Silva, C.M.S., Cavalheiro, M.F., Bressan, A.C.G., Carvalho, B.M.O., Banhos, O.F.A.A., Purgatto, E., Harakava, R., Tanaka, F.A.O., Habermann, G., 2019. Aluminum-induced high IAA concentration may explain the Al susceptibility in *Citrus limonia*. *Plant Growth Regul.* 87, 123–137.

Simon, L., Kieger, M., Sung, S.S., Smalley, T.J., 1994. Aluminum toxicity in tomato. Part 2. Leaf gas exchange, chlorophyll content, and invertase activity. *J Plant Nutr.* 17, 307–317.

Singh, S., Tripathi, D.K., Singh, S., Sharma, S., Dubey, N.K., Chauhan, D.K., Vaculík, M., 2017.

Toxicity of aluminium on various levels of plant cells and organism: A review. *Environ. Exp. Bot.* 137, 177–193.

Souza, T., Cambraia, J., Ribeiro, C., Oliveira, J.Á., Silva, L.C., 2016. Effects of aluminum on the elongation and external morphology of root tips in two maize genotypes. *Bragantia* 75, 19-25.

Sussmilch, F.C., Brodribb, T.J., McAdam, S.A.M., 2017. Up-regulation of NCED3 and ABA biosynthesis occur within minutes of a decrease in leaf turgor but AHK1 is not required. *J. Exp. Bot.* 68, 2913–2918.

Szatanik-Kloc, A., 2016. Changes in the size of the apparent surface area and adsorption energy of the rye roots by low pH and the presence of aluminum ions induced. *Int Agrophs.* 30, 375-381.

Tamás, L., Huttová, J., Mistrik, I., Simonovicová, M., Siroká, B., 2006. Aluminium-induced drought and oxidative stress in barley roots. *J. Plant Physiol.* 163, 781-784.

Tan, B-C., Joseph, L.M., Deng, W-T., Liu, L., Li, Q-B., Cline, K., McCarty, D.R., 2003. Molecular characterization of the *Arabidopsis* 9-*cis* epoxycarotenoid dioxygenase gene family. *Plant J.* 35, 44-56.

Thompson, A.J., Jackson, A.C., Symonds, R.C., Mulholland, B.J., Dadswell, A.R., Blake, P.S., Burbidge, A., Taylor I.B., 2000. Ectopic expression of a tomato 9-*cis*-epoxycarotenoid dioxygenase gene causes over-production of abscisic acid. *Plant J.* 23, 363–374.

Thompson, A.J., Andrews, J., Mulholland, B.J., McKee, J.M.T., Hilton, H.W., Horridge, J.S., Farquhar, G.D., Smeeton, R.C., Smillie, I.R.A., Black, C.R., Taylor, I.B., 2007. Overproduction of abscisic acid in tomato increases transpiration efficiency and root hydraulic conductivity and influences leaf expansion. *Plant Physiol.* 143, 1905–1917.

Turner N.C., 1981. Techniques and experimental approaches for the measurement of plant water status. *Plant Soil* 58, 339–366.

Vitorello, V.A., Capaldi, F.R., Stefanuto, V.A., 2005. Recent advances in aluminium toxicity and resistance in higher plants. *Braz. J. Plant Physiol.* 17, 129–143.

Weng, J.K., Ye, M., Li, B., Noel, J.P., 2016. Co-evolution of hormone metabolism and signaling networks expands plant adaptive plasticity. *Cell* 166, 881-893.

Xian, L., Sun, P., Hu, S., Wu, J., Liu, J-H., 2014. Molecular cloning and characterization of *CrNCED1*, a gene encoding 9-*cis*-epoxycarotenoid dioxygenase in *Citrus reshni*, with functions in tolerance to multiple abiotic stresses. *Planta* 239, 61-77.

Xiong, L., Zhu J., 2003. Regulation of Abscisic Acid Biosynthesis. *Plant Physiol.* 133, 29–36.

Xu, Z-Y., Kim, D.H., Hwang, I., 2013. ABA homeostasis and signaling involving multiple subcellular compartments and multiple receptors. *Plant Cell Rep.* 32, 807–813.

Yang, Z., Rao, I.M., Horst, W.J., 2013. Interaction of aluminium and drought stress on root growth and crop yield on acid soils. *Plant Soil* 372, 3–25.

Yang, Z-B., Liu, G., Liu, J., Zhang, B., Meng, W., Müller, B., Hayashi, K-i., Zhang, X., Zhao, Z., De Smet, I., Ding, Z., 2017. Synergistic action of auxin and cytokinin mediates aluminum-induced root growth inhibition in *Arabidopsis*. *EMBO Rep.* 7, 1213-1230.

- Zaharia, L.I., Walker-Simmon, M.K., Rodríguez, C.N., Abrams, S.R., 2005. Chemistry of abscisic acid, abscisic acid catabolites and analogs. *J. Plant Growth Regul.* 24, 274–284
- Zhao, S., Fernald, R.D., 2005. Comprehensive algorithm for quantitative real-time polymerase chain reaction. *J. Computl. Biol* 12, 1047–1064.
- Zhang, J., Davies, W.J., 1989. Abscisic acid produced in dehydrating roots may enable the plant to measure the water status of the soil. *Plant Cell Environ.* 12, 73–81.
- Zhang, Y., Yang, J., Lu, S., Cai, J., Guo, Z., 2008. Overexpressing SgNCED1 in tobacco increases ABA level, antioxidant enzyme activities, and stress tolerance. *J. Plant Growth Regul.* 27, 151–158.
- Zhang, F.P., Susmilch, F., Nichols, D.S., Cardoso, A.A., Brodribb, T.J., McAdam, S.A.M., 2018. Leaves, not roots or floral tissue, are the main site of rapid, external pressure-induced ABA biosynthesis in angiosperms. *J. Exp. Bot.* 69, 1261–1267.
- Zandalinas, S.I., Rivero, R.M., Martínez, V., Gómez-Cadenas, A., Arbona, V., 2016. Tolerance of citrus plants to the combination of high temperatures and drought is associated to the increase in transpiration modulated by a reduction in abscisic acid levels. *BMC Plant Biol.* 16, 105.

Tables

Table 1. List of gene primers used for qRT-PCR analysis in *Citrus limonia*.

Gene abbreviation	Gene name	Forward (5'-3')	Reverse (5'-3')	References
GAPC2	Glyceraldehyde-3-phosphate dehydrogenase	5'-TCCTATGTTTGTGTTGGGTG-3'	5'-GGTCATCAAACCCTCAACAA-3'	Mafra <i>et al.</i> , 2012; Silva <i>et al.</i> , 2019
EF α	Elongation factor 1-alpha	5'-TCAGGCAAGGAGCTTGAGAAG-3'	5'-GGCTTGGTGGGAATCATCTTAA-3'	Mafra <i>et al.</i> , 2012; Silva <i>et al.</i> , 2019
NCED1	9-cis-epoxycarotenoid dioxygenase 1	5'-GACCAGC AAGTGGTGTTCAA-3'	5'-AGAGGTGAAACAGGAGCAA-3'	Bassene <i>et al.</i> , 2009; Neves <i>et al.</i> , 2013
NCED3	9-cis-epoxycarotenoid dioxygenase 3	5'-GGAGAATGAGGATGATGGCTAC-3'	5'-CTTTCGCGCTTATGAACGTG-3'	Agusti <i>et al.</i> , 2007; Neves <i>et al.</i> , 2013
NCED5	9-cis-epoxycarotenoid dioxygenase 5	5'-CTTCCCAACGAAGT CCATAG-3'	5'-GGATTCCATTGTGATTGCTG-3'	Agusti <i>et al.</i> , 2007; Neves <i>et al.</i> , 2013

Figure legends

Fig. 1. Main root length (A), root surface area (B), root diameter (C) and root biomass (D) of *C. limonia* grown for 90 days in nutrient solution containing 0 and 1480 μM Al. For each evaluation date, asterisks indicate significant differences ($P < 0.05$) between 0 and 1480 μM Al. For plants not exposed to Al, distinct uppercase letters indicate significant differences ($P < 0.05$) between 0 and 90 DAT; for plants exposed to Al, distinct lowercase letters indicate significant differences ($P < 0.05$) between 0 and 90 DAT. Columns are mean values ($n = 6, \pm \text{SE}$).

Fig. 2. Leaf number (A), area (B) and biomass (C) of *C. limonia* grown for 90 days in nutrient solution containing 0 and 1480 μM Al. For each evaluation date, asterisks indicate significant differences ($P < 0.05$) between 0 and 1480 μM Al. For plants not exposed to Al, distinct uppercase letters indicate significant differences ($P < 0.05$) between 0 and 90 DAT; for plants exposed to Al, distinct lowercase letters indicate significant differences ($P < 0.05$) between 0 and 90 DAT. Columns are mean values ($n = 6, \pm \text{SE}$).

Fig. 3. Leaf gas exchange and water use efficiency of *C. limonia* grown for 90 days in nutrient solution containing 0 and 1480 μM Al. (A) CO_2 assimilation, (B) stomatal conductance, (C) transpiration, (D) intercellular CO_2 , (E) water use efficiency and (F) intrinsic water use efficiency. For each evaluation date, asterisks indicate significant differences ($P < 0.05$) between 0 and 1480 μM Al. Circle symbols are mean values ($n = 6, \pm \text{SE}$).

Fig. 4. Leaf water potential at predawn (Ψ_{pd}) (A) and midday (Ψ_{md}) (B) of *C. limonia* grown for 90 days in nutrient solution containing 0 and 1480 μM Al. For each evaluation date, asterisks indicate significant differences ($P < 0.05$) between 0 and 1480 μM Al. Circle symbols are mean values ($n = 4, \pm \text{SE}$).

Fig. 5. Relative leaf water content (A) and estimated hydraulic conductance from roots to the leaf (B) of *C. limonia* grown for 90 days in nutrient solution containing 0 and 1480 μM Al. For each evaluation date, asterisks indicate significant differences ($P < 0.05$) between 0 and 1480 μM Al. Circle symbols are mean values ($n = 6, \pm \text{SE}$).

Fig. 6. Foldchange of normalized expression level of *CINCED1*, *CINCED3* and *CINCED5* in leaves (A, C, E, respectively) and root tips (B, D, F, respectively) of *C. limonia* grown for 90 days in nutrient solution containing 0 and 1480 μM Al. For each evaluation date, asterisks indicate significant differences ($P < 0.05$) between 0 and 1480 μM Al. The dotted line represents the control group, showing always the mean value of 1, and foldchange is that between control and Al treatment. Circle symbols are mean values ($n = 4, \pm \text{SE}$).

Fig. 7. Abscisic acid (ABA) and its metabolites in leaves (left columns) and roots (right columns) of *C. limonia* grown for 90 days in nutrient solution containing 0 and 1480 μM Al. For each evaluation date, asterisks indicate significant differences ($P < 0.05$) between 0 and 1480 μM Al. Circle symbols are mean values ($n = 4, \pm \text{SE}$). (PA: phaseic acid; DPA: dihydrophaseic acid; 7'OHABA: (+)-7'-hydroxy-abscisic acid; ABA-GE: abscisic acid glucosyl ester).

Fig 8. Aluminum concentration in leaves (A) and roots (B) of *C. limonia* grown for 90 days in nutrient solution containing 0 and 1480 μM Al. For each evaluation date, asterisks indicate significant differences ($P < 0.05$) between 0 and 1480 μM Al. For plants not exposed to Al, distinct uppercase letters indicate significant differences ($P < 0.05$) between 0 and 90 DAT; for plants exposed to Al, distinct lowercase letters indicate significant differences ($P < 0.05$) between 0 and 90 DAT. Columns are mean values ($n = 6, \pm \text{SE}$).

Appendix A. Supplementary data

Additional supporting information may be found in the online version of this article.

Fig. S1. Morphological details of shoots, leaves and roots of *C. limonia* grown for 90 days in nutrient solution containing 0 (on the left) and 1480 μM Al (on the right).

Fig. S2. Individual readings (replicates; $n = 4$ plants) of leaf abscisic acid concentration ($[\text{ABA}]_{\text{leaf}}$) and *CINCED3* expression (Foldchange) in *C. limonia* grown for 90 days in nutrient solution containing 1480 μM Al.

Fig. S3. Individual readings (replicates; $n = 4$ plants) of leaf abscisic acid concentration ($[\text{ABA}]_{\text{leaf}}$) and stomatal conductance (g_s) in *C. limonia* grown for 90 days in nutrient solution containing 0 and 1480 μM Al.

Highlights:

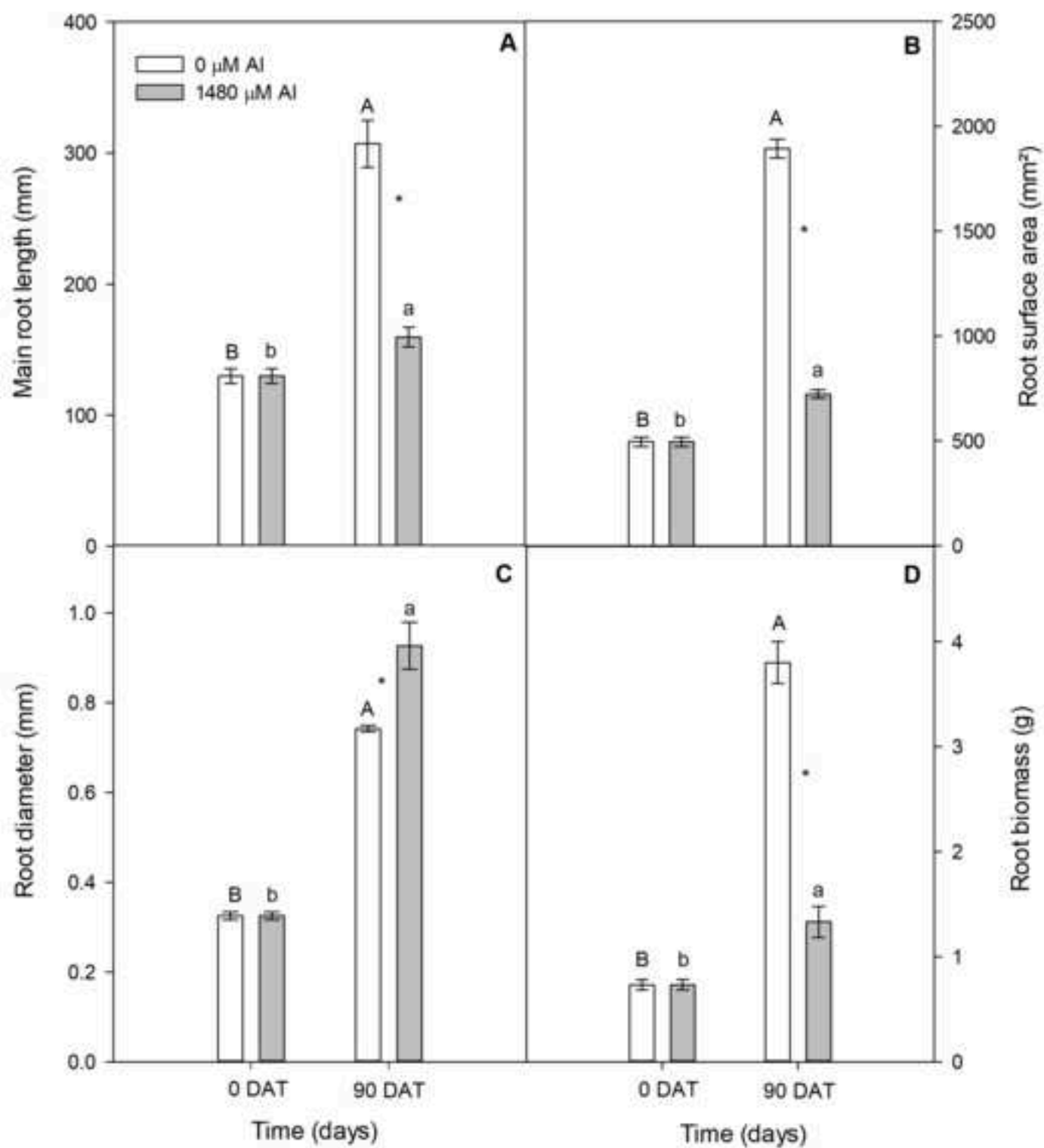
Aluminum (Al) toxicity inhibits root growth and reduces the stomatal conductance (*gs*)

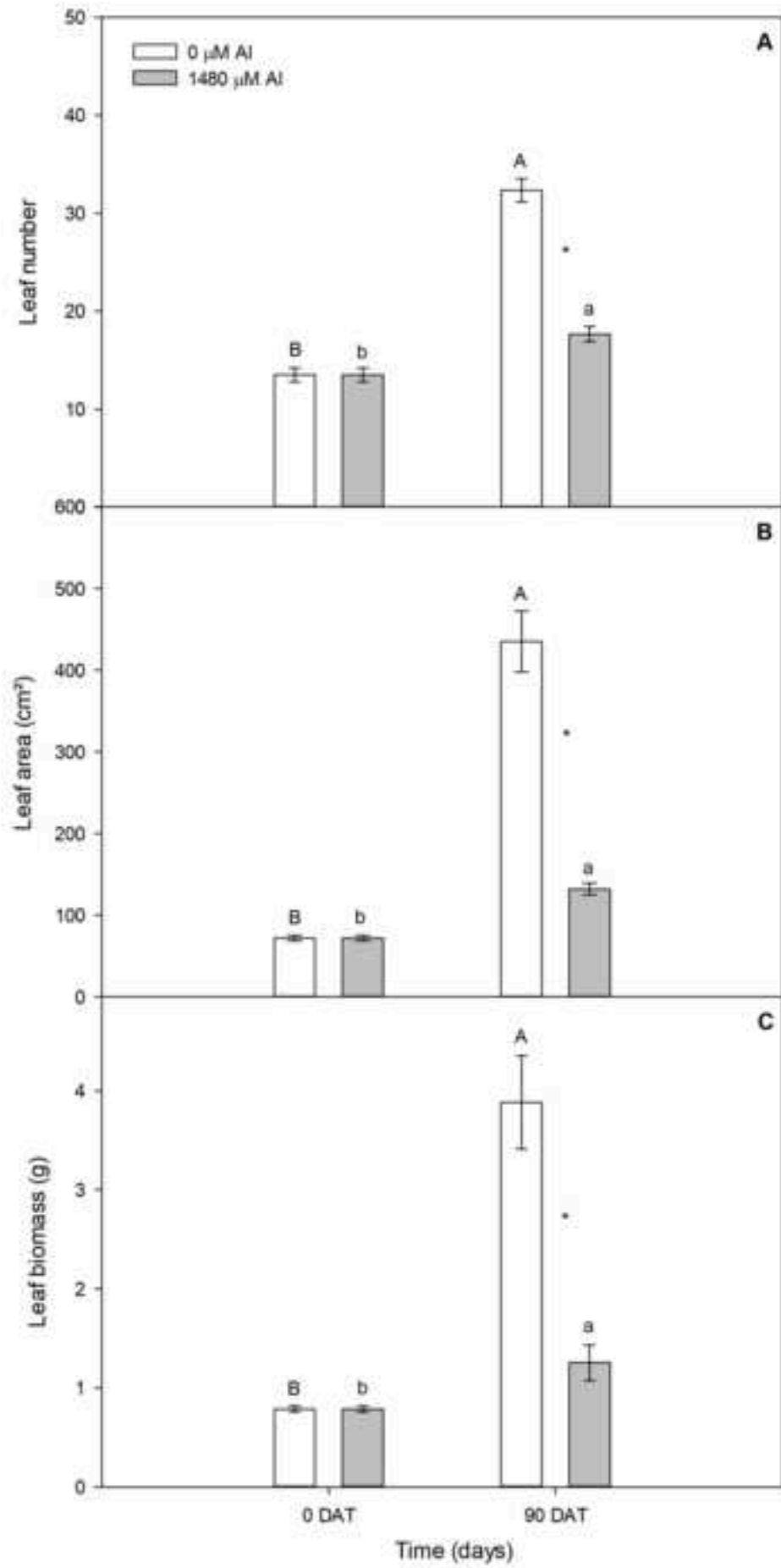
The 9-*cis*-epoxycarotenoid dioxygenase (NCED) enzyme catalyzes the abscisic acid (ABA)

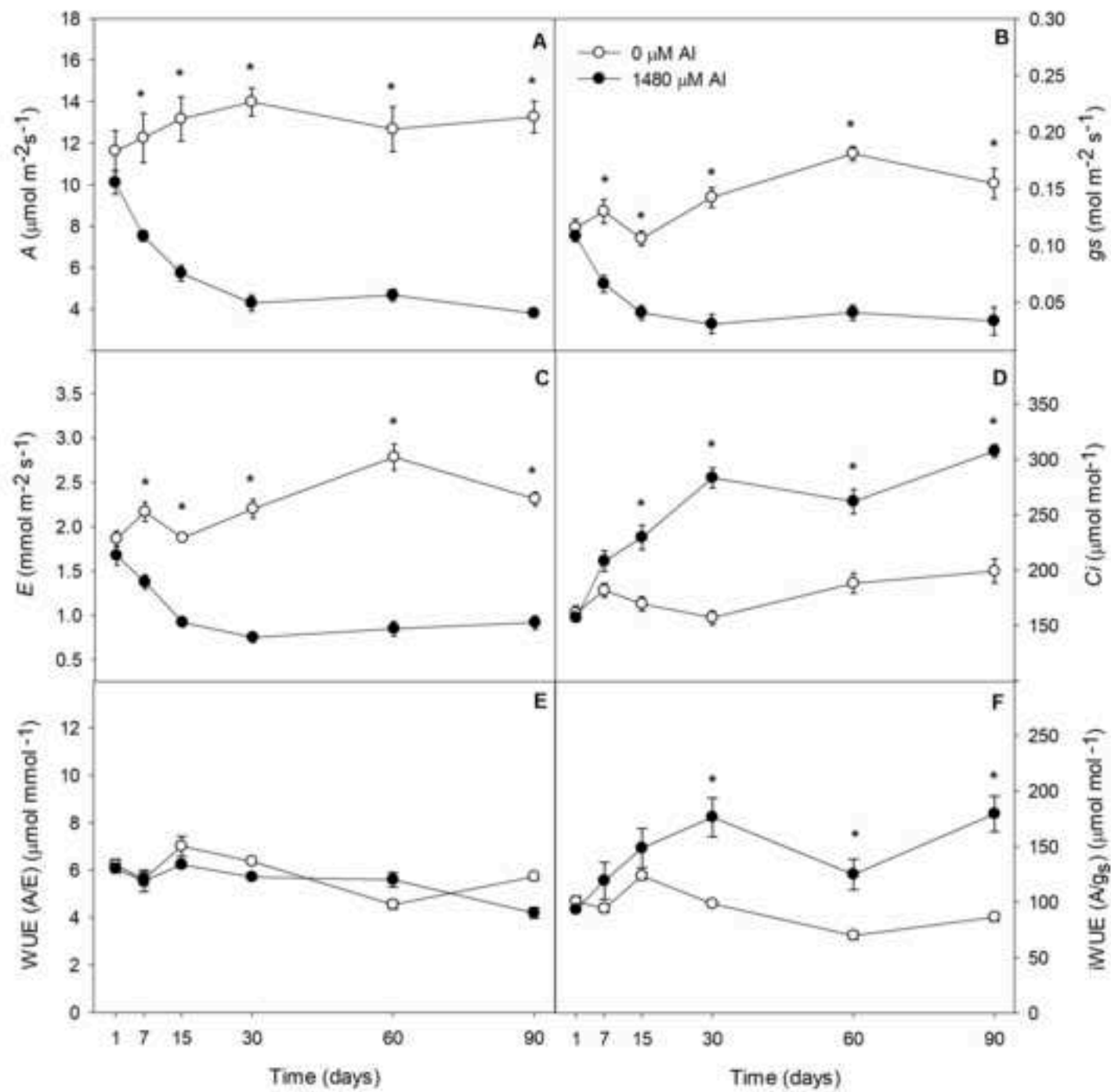
Roots of *Citrus limonia* exposed to Al up-regulated *CINCED3* before *gs* was reduced

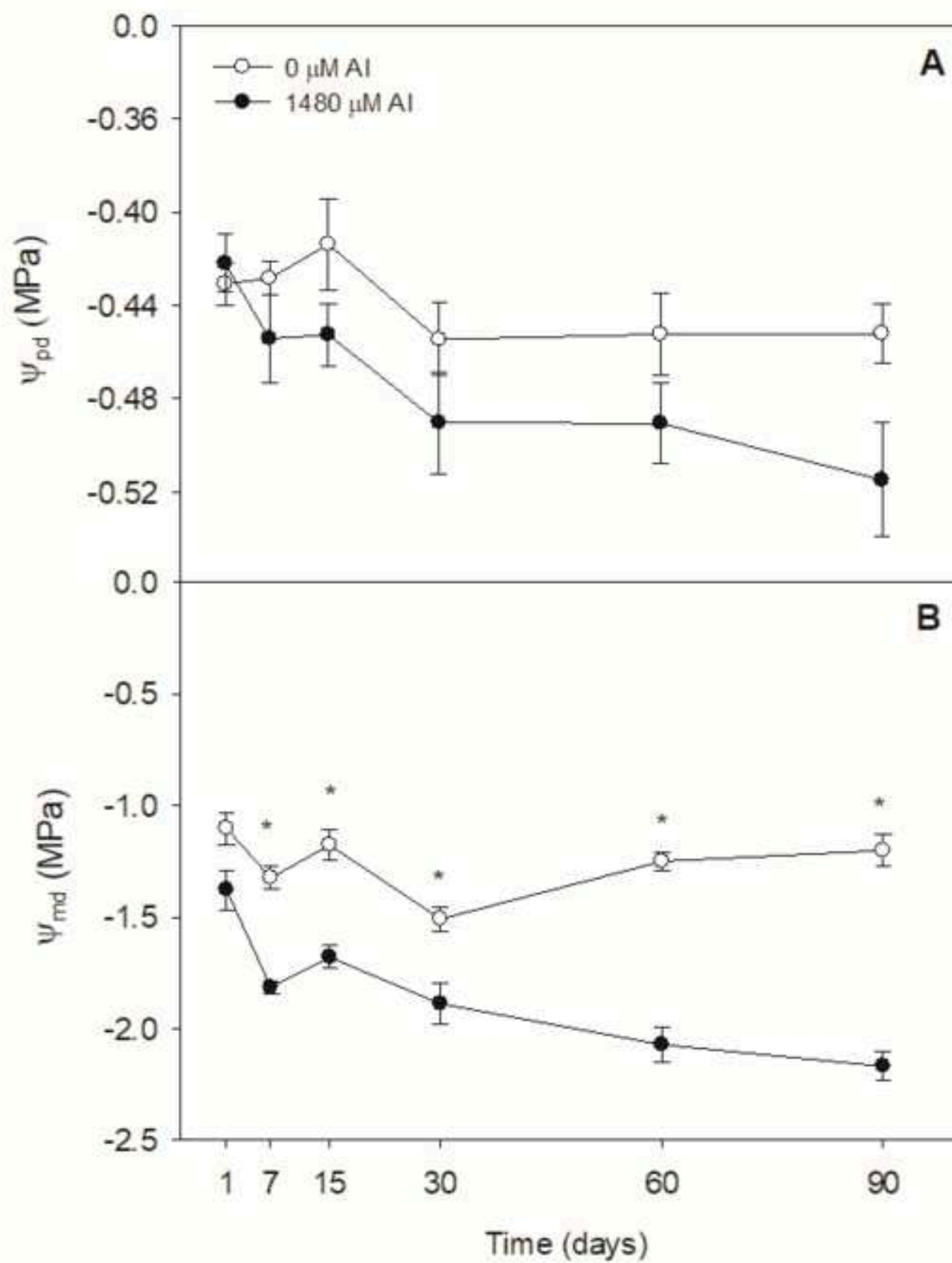
Up-regulation of *CINCED3*, *CINCED1* and *CINCED5* matched ABA leaf levels

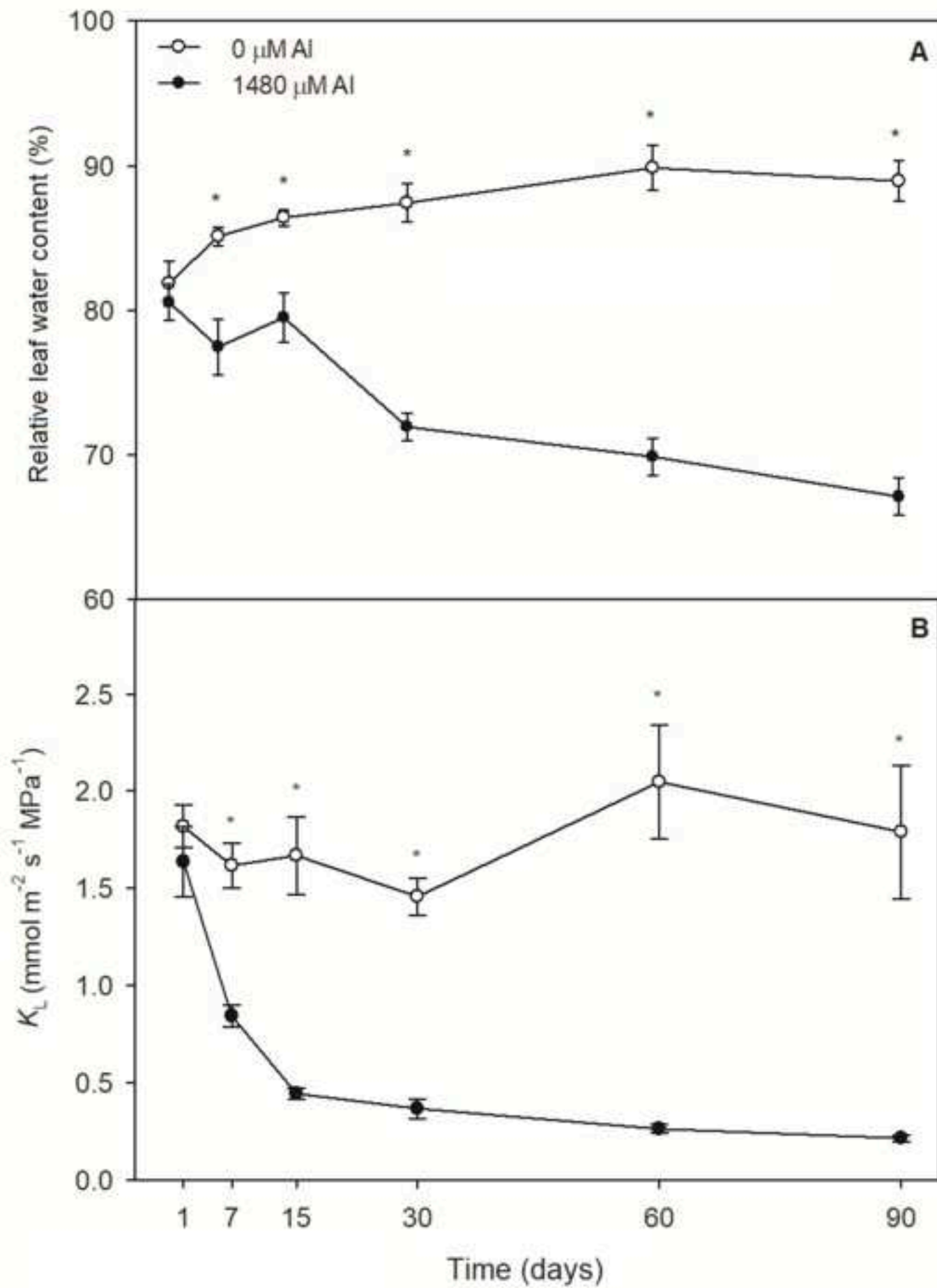
Al triggers ABA biosynthesis, which is associated with the low *gs*

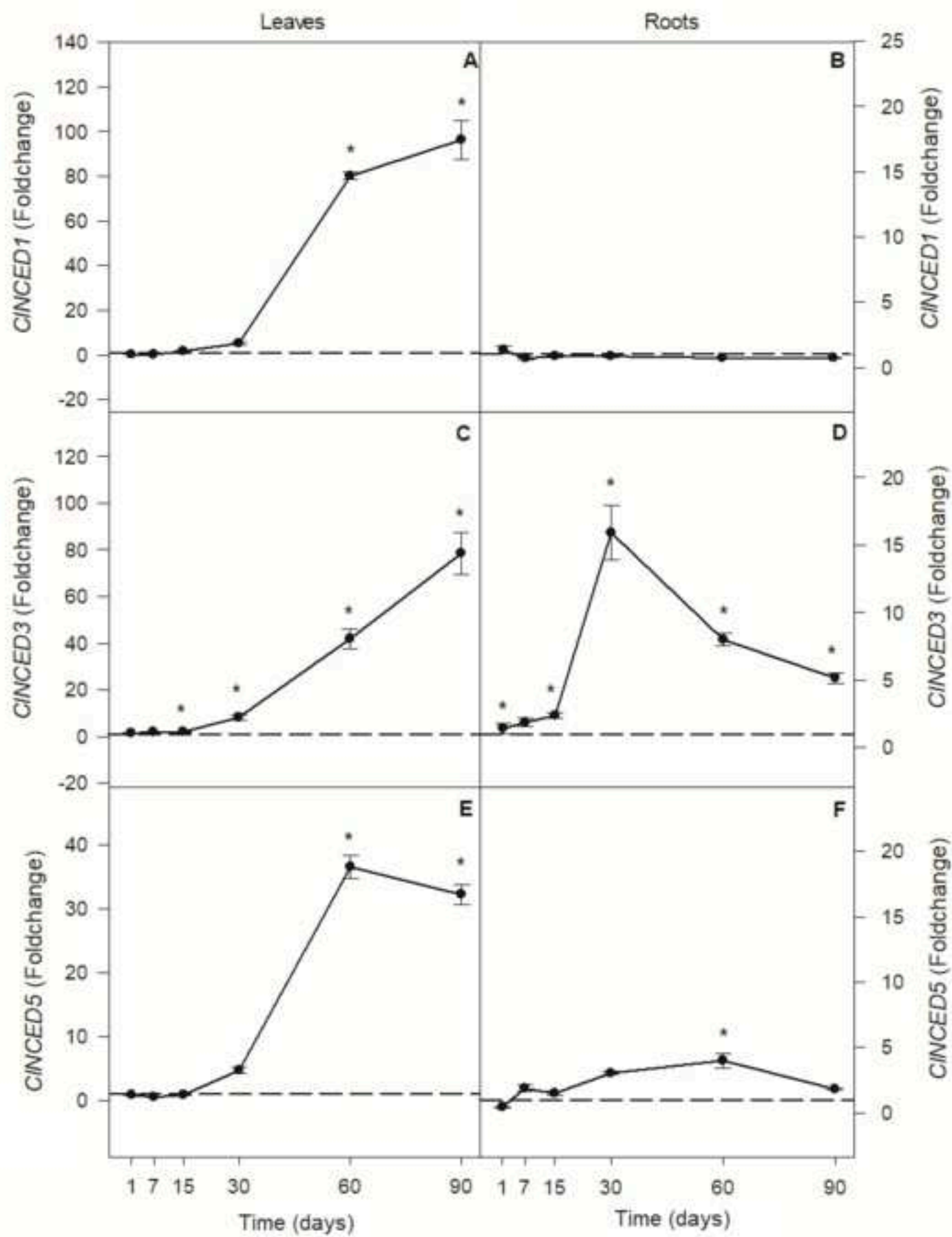


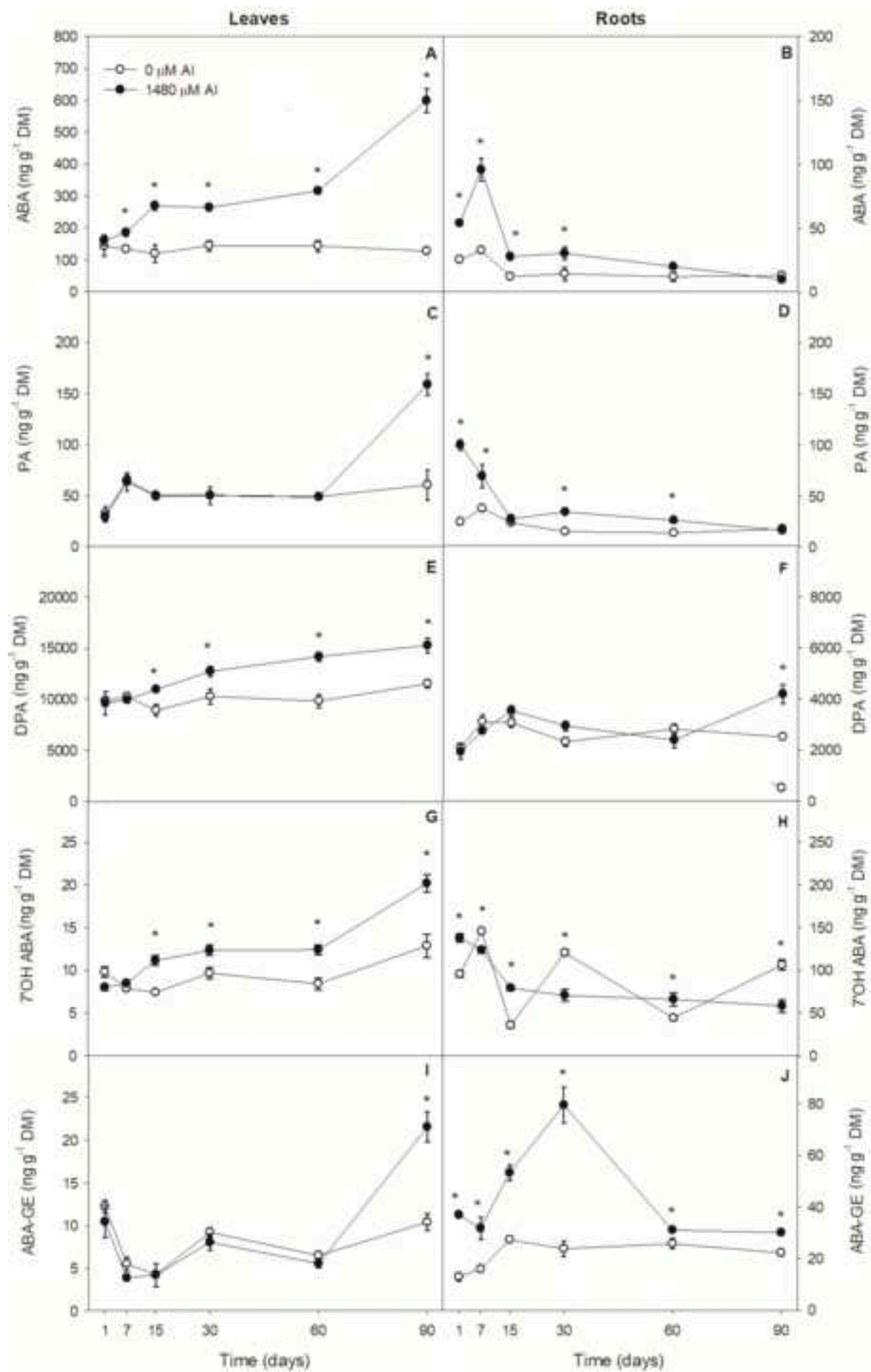


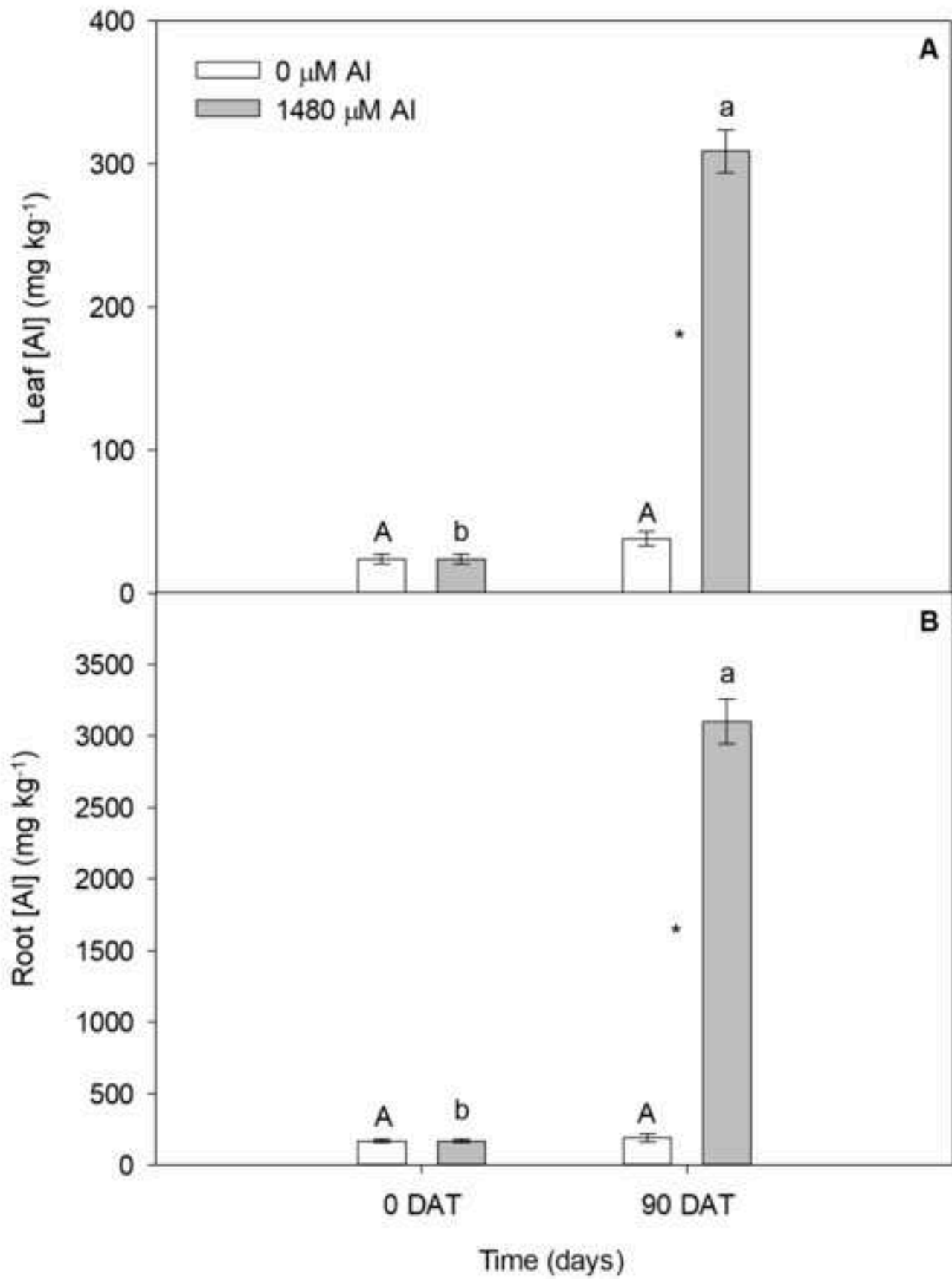




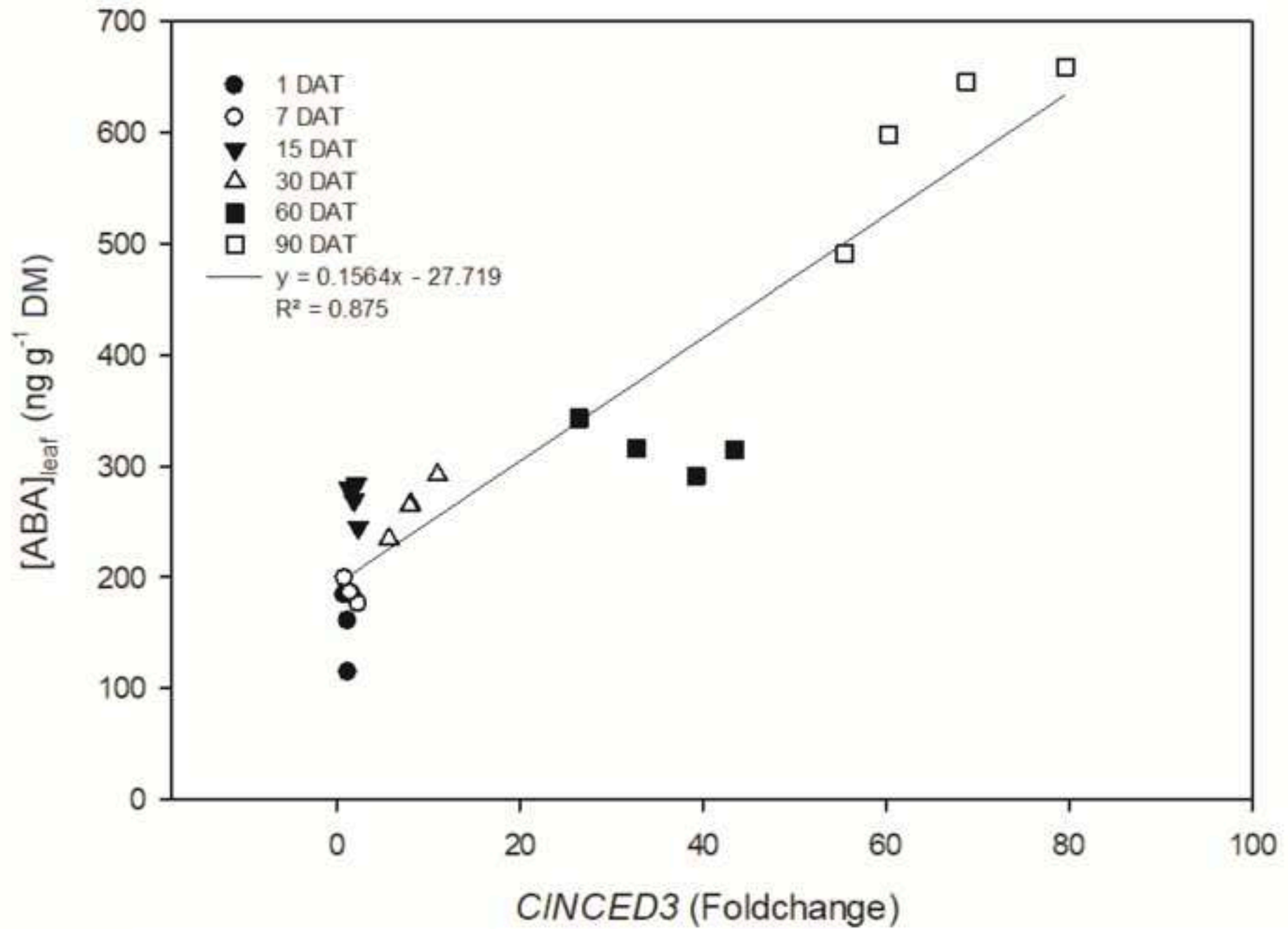


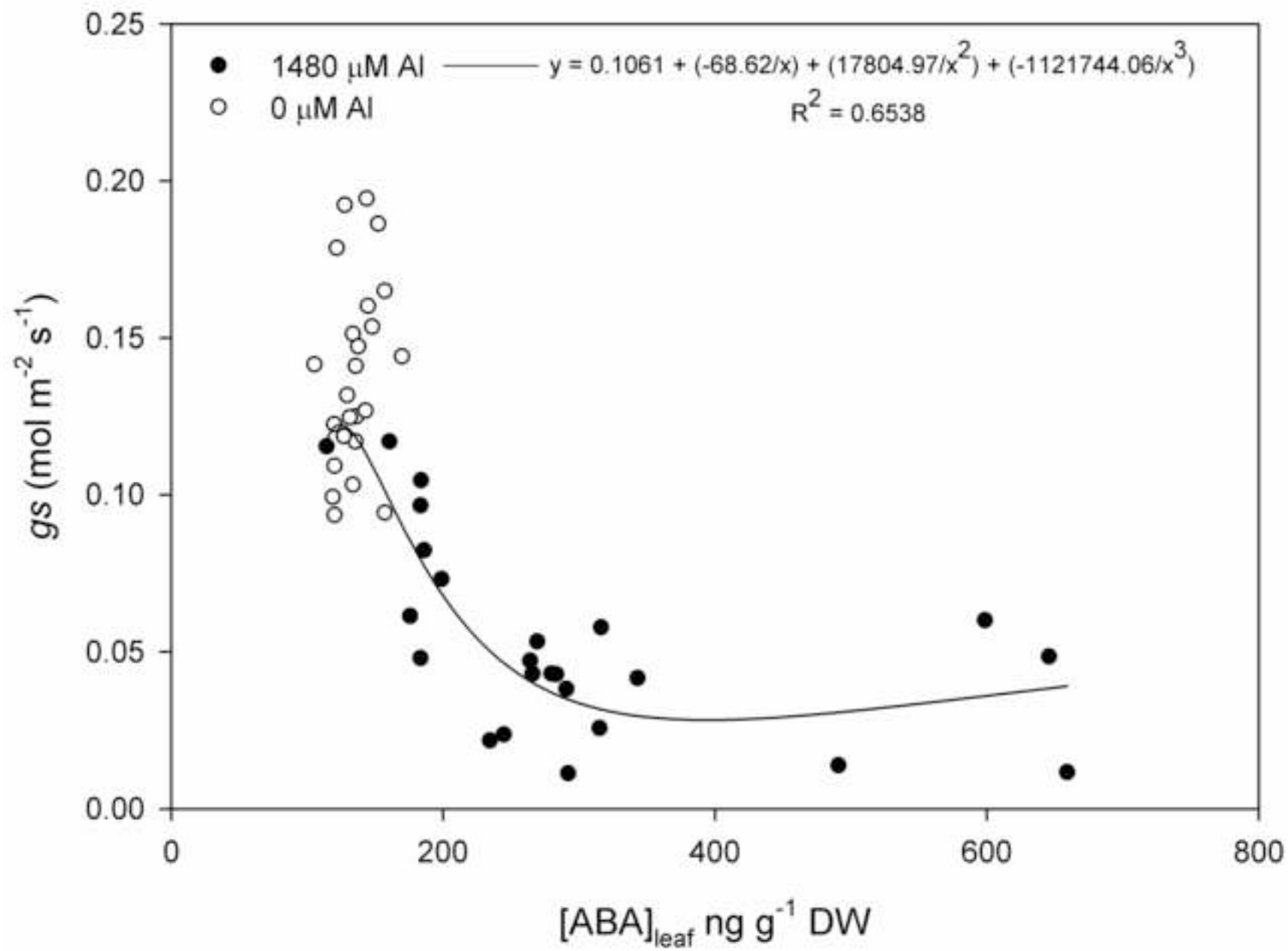












NCED expression is related to increased ABA biosynthesis and stomatal closure under aluminum stress

Gavassi, Marina Alves

2021-01-30

Attribution-NonCommercial-NoDerivatives 4.0 International

Gavassi MA, Silva GS, da Silva CD, et al., (2021) NCED expression is related to increased ABA biosynthesis and stomatal closure under aluminum stress. *Environmental and Experimental Botany*, Volume 185, May 2021, Article number 104404

<https://doi.org/10.1016/j.envexpbot.2021.104404>

Downloaded from CERES Research Repository, Cranfield University